Lineal Confocal-OCT

Josep Malvehy

Hospital Clinic of Barcelona, Spain

Clínic Barcelona

IDIBAPS

Institut D'Investigacions Biomèdiques August Pi i Sunyer

Conflicts

SPEAKER: Almirall, BMS, ISDIN, La Roche Posay, Leo, Novartis, Pierre Fabre, Roche, Sanofi

HONORARIA OR CONSULTATIONS FEES : Almirall, BMS, Biofrontera, GSK, ISDIN, La Roche Posay, Leo, Novartis, Polychem

GRANTS & RESEARCH SUPPORT: Almirall, Amgen, BMS, Biofrontera, Canfield, Cantabria, Fotofinder,

GSK, ISDIN, La Roche Posay, Leo, Mavig, Nevisense, Novartis, Polychem, Roche, iTOBOs (EU Grant), Castle Biosciences, NelaCare, and SkylineDx, Amlo Bioscience

Spouse/partner: Almirall, Amgen, BMS, Biofrontera, Canfield, Cantabria, Fotofinder, GSK, ISDIN, La Roche Posay, Leo, Mavig, Nevisense, Novartis, Pierre Fabre, Polychem, Roche

Other support (please specify): Abbie (educational activities), Lilly (educational activities), Novartis

Co-founder of Diagnosis Dermatologica sl and Athena Care sl.

ATHENA TECH

DIAGNOSIS DERMATOLOGICA

Clínic Barcelona

FOUNDING & COLLABORATIONS

New imaging technology in skin cancer

IN VIVO CONFOCAL MICROSCOPY

MULTIPHOTON MICROSCOPY

OPTICAL COHERENCE TOMOGRAPHY

HIGH FREQUENCY ULTRASOUND

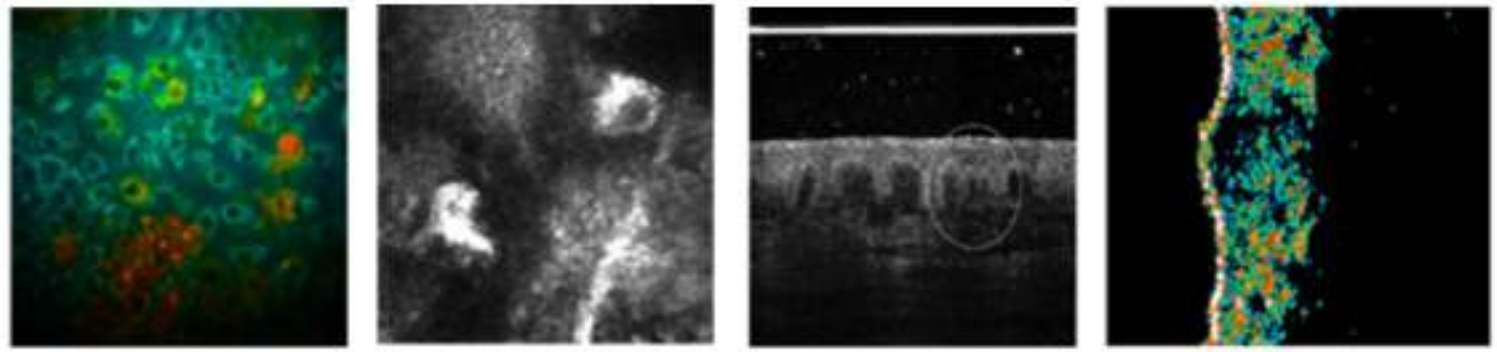

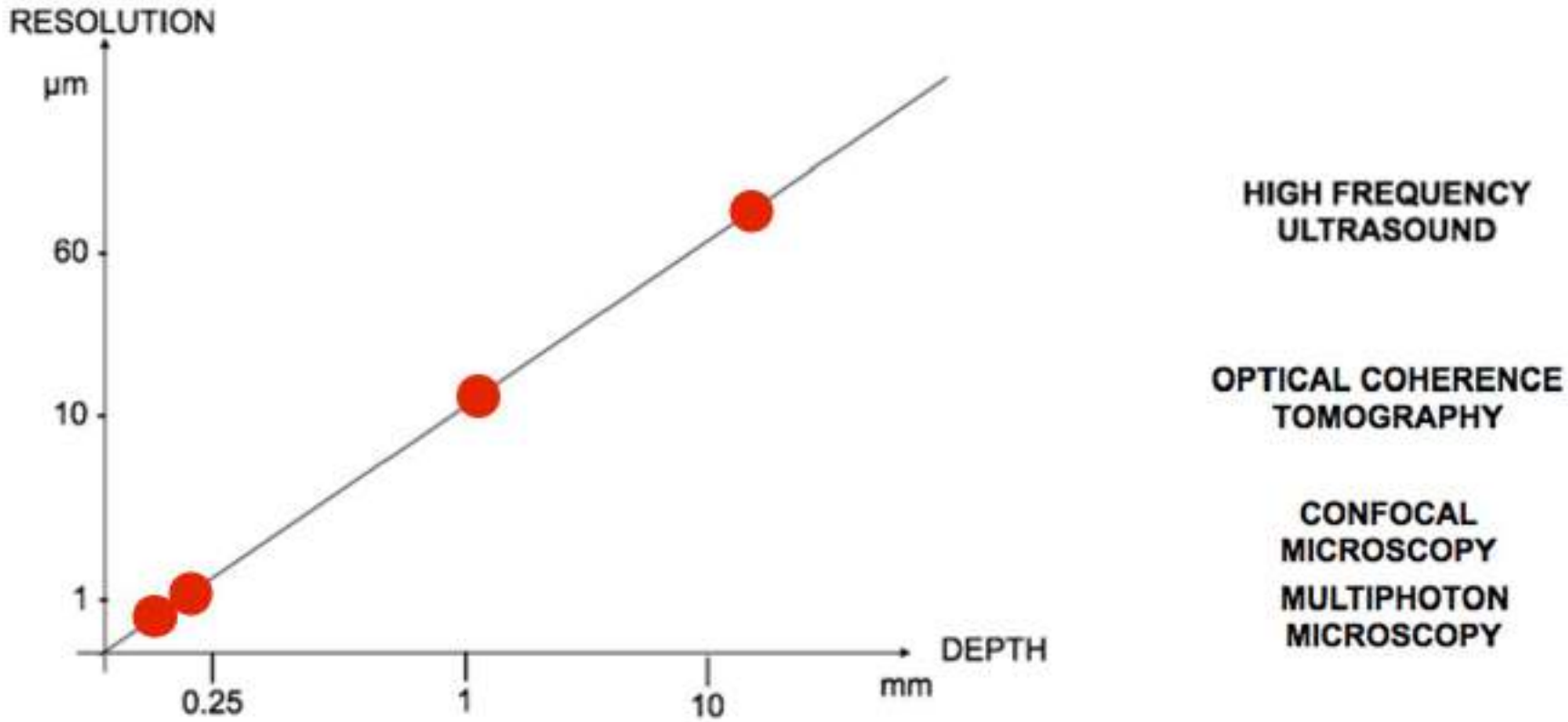

Courtesy of Giovanni Pellacani

Technical characteristics of RCM and OCT microscopes with clinical applicability

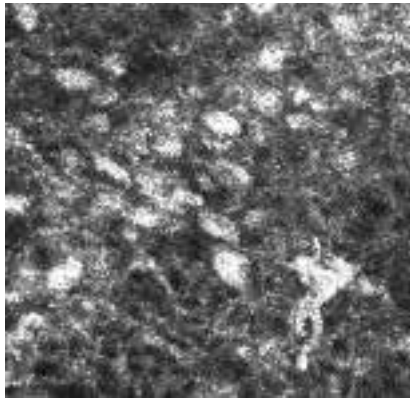

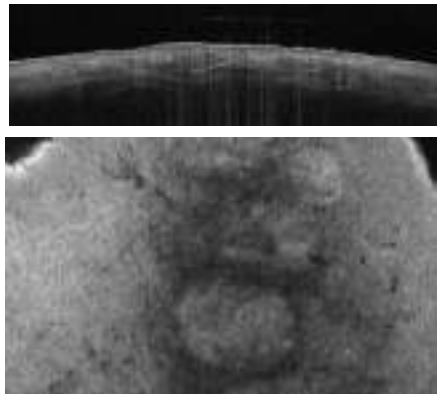

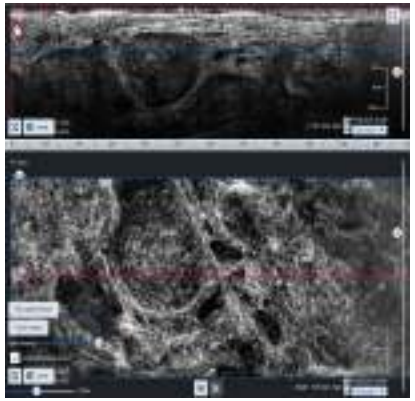

	RCM	OCT	LF-OCT
Horizontal (en face)	Yes	Yes	Yes
Vertical (slice, cross-sectional)	No	Yes (3D)	Yes (3D)
Depth	250 µm	2000 µm	500 µm
Lateral resolution	1 µm	7.5 µm	1 µm
Axial resolution	3 µm	10 µm	1 µm
Cellular resolution	**Yes**	**No**	**Yes**
Time exam	1-5 min	1 min	1-5 min
Field of view	500x500 µm 750x750 µm Vivablocks 8x8 mm	6 x 6 mm	1,2 x 0,5 mm

Journal of Biomedical Optics

BiomedicalOptics.SPIEDigitalLibrary.org

Line-field confocal optical coherence tomography for high-resolution noninvasive imaging of skin tumors

Arnaud Dubois
Olivier Levecq
Hicham Azimani
David Siret
Anaïs Barut
Mariano Suppa
Véronique del Marmol
Josep Malvehy
Elisa Cinotti
Pietro Rubegni
Jean-Luc Perrot

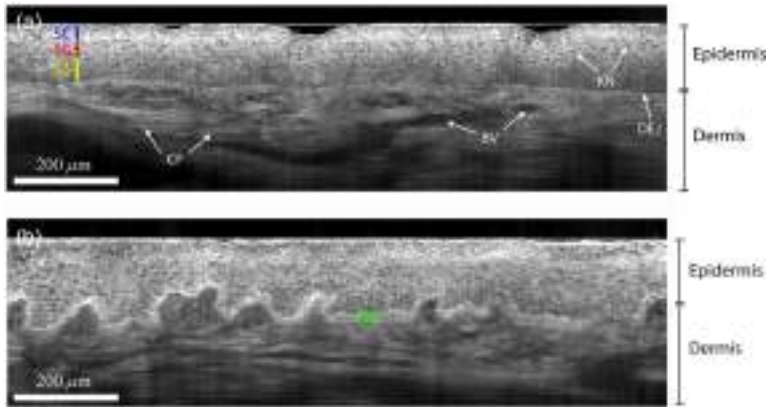

LC-OCT measures the echo-time delay and amplitude of light back scattered from cutaneous microstructures through low-coherence interferometry associated with confocal spatial filtering.

Arnaud Dubois, Olivier Levecq, Hicham Azimani, David Siret, Anaïs Barut, Mariano Suppa, Véronique del Marmol, Josep Malvehy, Elisa Cinotti, Pietro Rubegni, Jean-Luc Perrot, "Line-field confocal optical coherence tomography for high-resolution noninvasive imaging of skin tumors," *J. Biomed. Opt.* **23**(10), 106007 (2018), doi: 10.1117/1.JBO.23.10.106007.

Line-field Confocal Optical Coherence Tomography (LC-OCT)

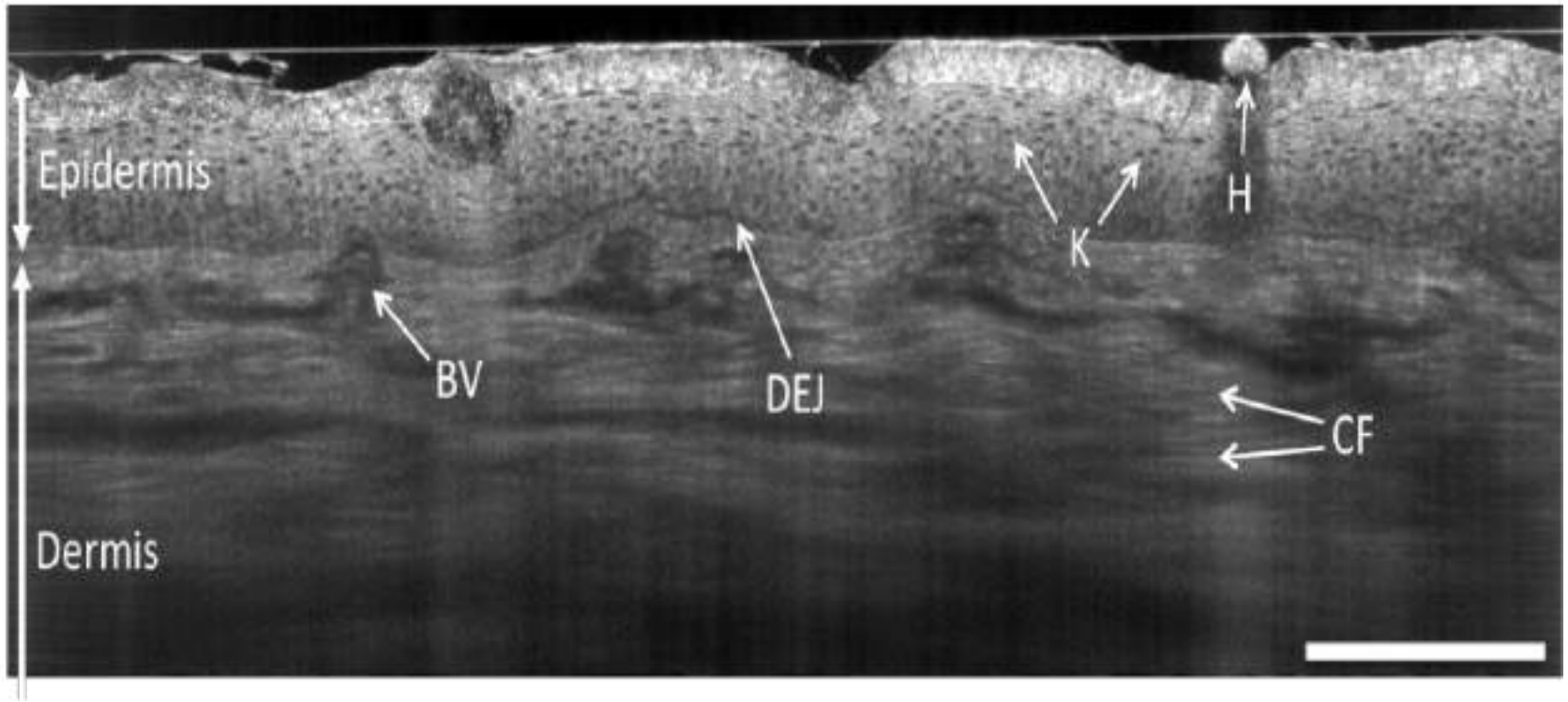

B-scan image of healthy human skin (back of the hand), obtained with OCTAV® (Scale bar: 200µm)

Line-field Confocal Optical Coherence Tomography (LC-OCT)

Basal cell carcinoma

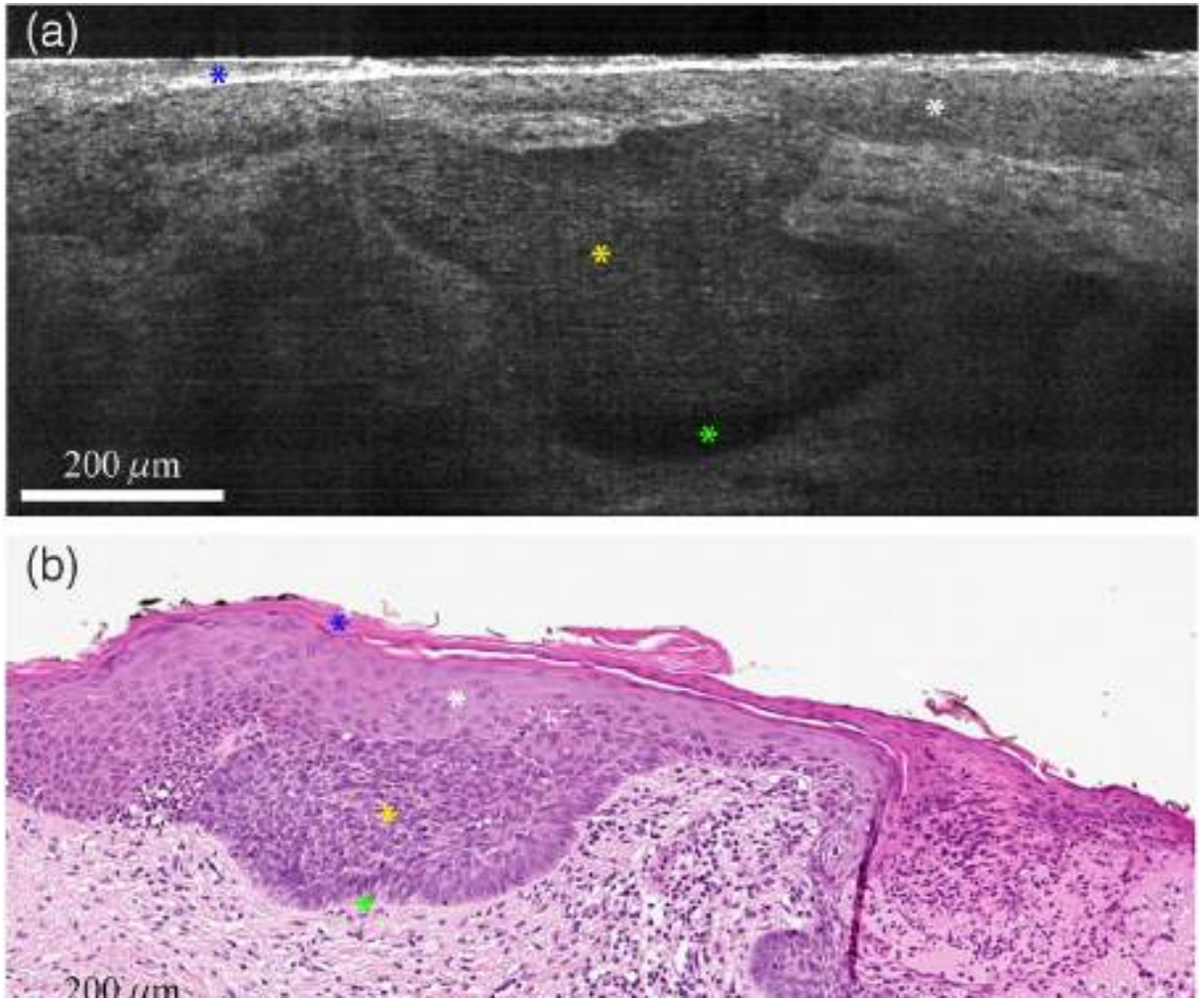

Melanoma

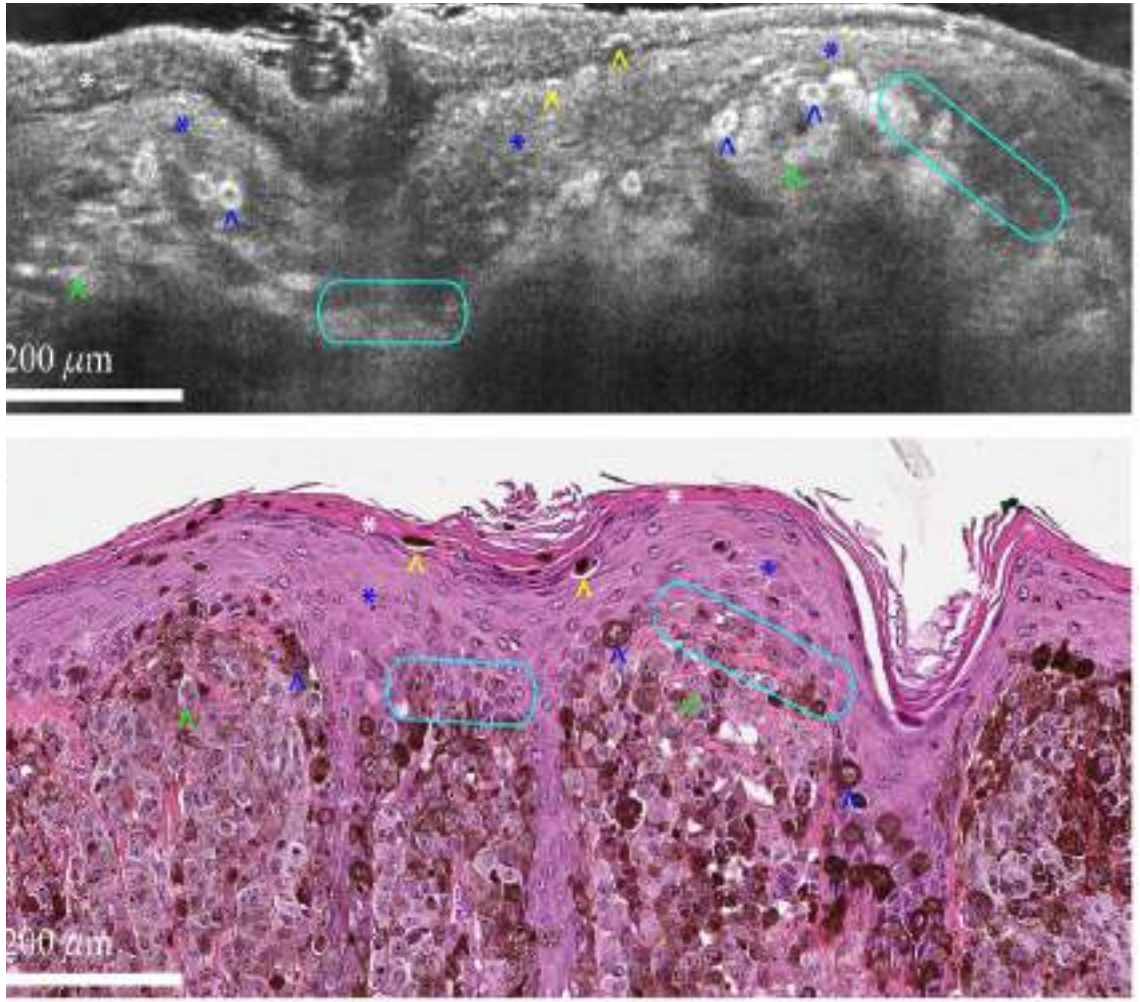

Consortium for research in LC-OCT

Hôpital Erasme – ULB
Veronique del Marmol
Mariano Suppa
Jovanie Razafindrakoto
Florence Bourlond

Hôpital St Etienne
Jean Luc Perrot

Hosp.Clínic Barcelona
Josep Malvehy
Susana Puig
Javiera Pérez
Pau Roses

University of Siena, S. Maria alle Scotte Hospital
Pietro Rubegni
Elisa Cinotti
L. Tognetti

DAMAE
Maxime Cazalas
Clothilde Raoux
Nicolas Linard

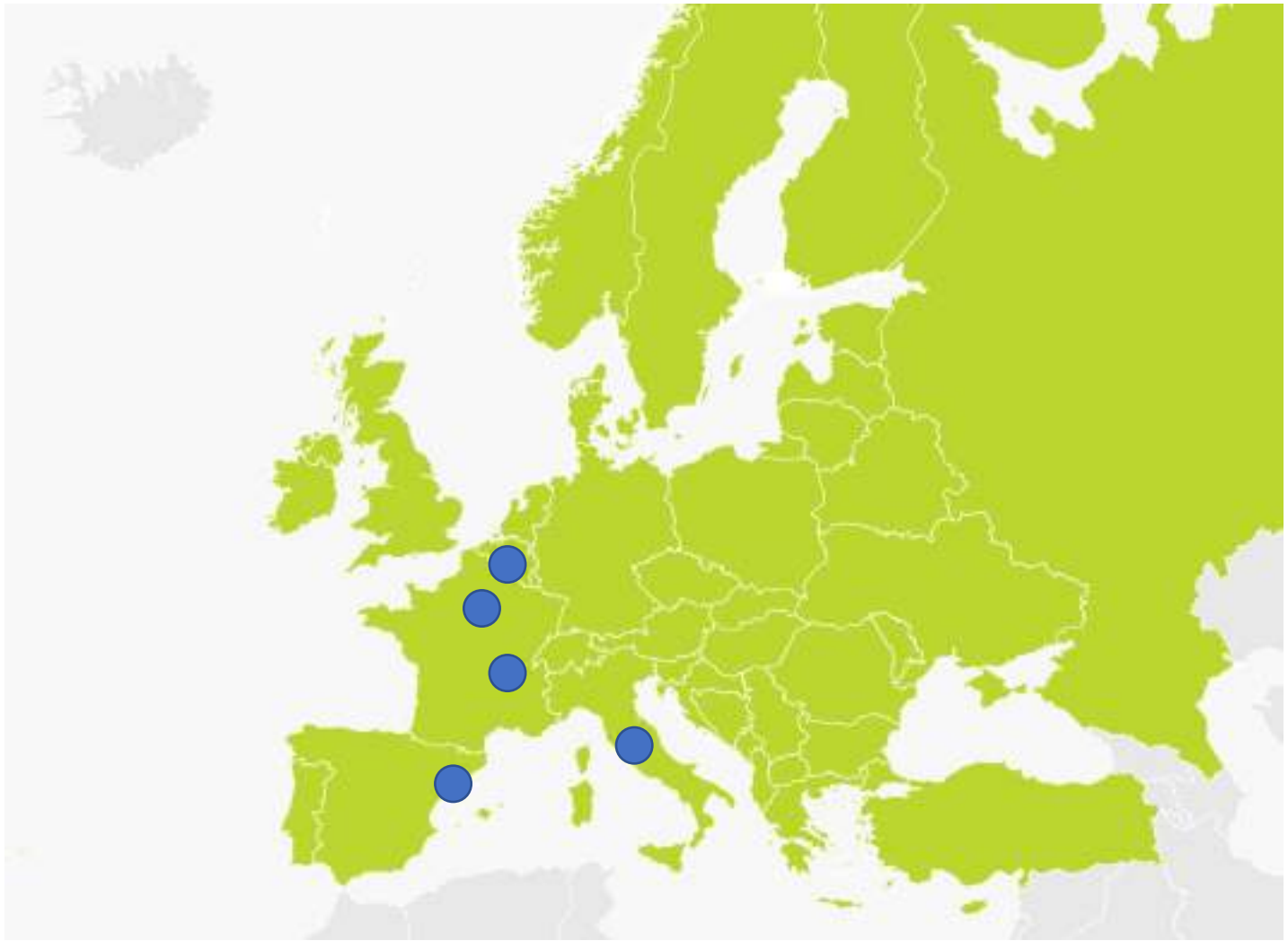

Consortium for research in LF- OCT

DAMAE
Anaïs Barut, DAMAE Medical affairs
Maxime Cazalas, DAMAE, innovation manage
Nicolas Linard, Medical department DAMAE

Hôpital Erasme – ULB
Veronique del Marmol, Dermatology Department
Makiko Miyamoto, Dermatology Department
Mariano Suppa, Dermatology Department
Jovanie Razafindrakoto, Dermatology Department
Florence Bourlond, Dermatology Department

Hôpital St Etienne
Jean Luc Perrot, Dermatology Department

Hosp.Clínic Barcelona
Josep Malvehy, Dermatology Department
Susana Puig, Dermatology Department
Alicia Barreiro, Dermatology Department
Jilliane Monnier, Dermatology Department
Javiera Pérez, Dermatology

University of Siena, S. Maria alle Scotte Hospital
Pietro Rubegni, Dermatology Department
Elisa Cinotti, Dermatology Department
L. Tognetti, Dermatology Department

- Description of Healthy skin
- Evaluation of features in BCC, AK, SCC
- Evaluation of melanocytic lesions
- Other tumours
- Inflammatory diseases
- Comparison and combination with other techniques

In vivo Line Field-OCT

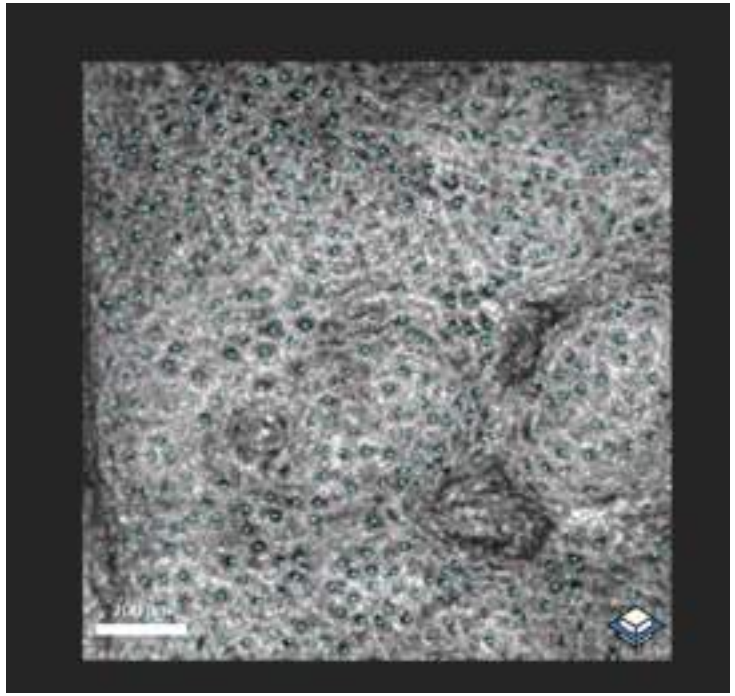

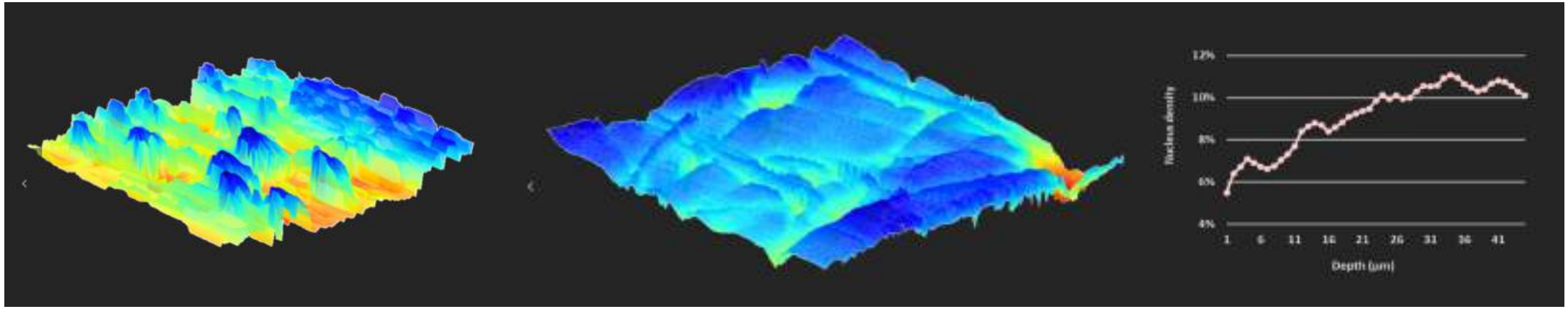

In vivo characterization of healthy human skin with a novel, non-invasive imaging technique: line-field confocal optical coherence tomography

Methods

Seven body sites (back of the hand, forehead, cheek, nose, chest, forearm and back) were investigated.

An independent qualitative [cutaneous structures' description; visibility of keratinocytes' nuclei and dermal–epidermal junction (DEJ)] and quantitative [stratum corneum (SC)/epidermal thicknesses; height of dermal papillae] assessment of the LC-OCT images was performed.

Results

A total of 88 LC-OCT images were collected from 29 participants (20 females; nine males; mean age 25.9 years). Keratinocytes' nuclei and DEJ were visible in the totality of images. The different layers of the epidermis and the remaining cutaneous structures/findings were visualized. Body sites-related variability was detected for SC/epidermal thicknesses and height of dermal papillae. Inter-observer agreement was excellent (SC thickness), good-to-excellent (epidermal thickness) and moderate-to-good (papillae).

Conclusions

Line-field confocal-OCT provides non-invasive, real-time imaging of the skin in vivo with deep penetra- tion and high resolution, enabling the visualization of single cells. The histology-like vertical view provides an easy way to recognize/measure different cutaneous structures/findings. LC-OCT appears as a promising technique for the examination of physiological/pathological skin.

Table 1 Quantitative evaluation of the skin at different body sites by means of line-field confocal optical coherence tomography (LC-OCT) images

Body site	Stratum corneum thickness (%)	Epidermal thickness (%)	Height of dermal papillae (%)
Forehead	11.6 ± 1.7 (15)	81.1 ± 12.9 (16)	18.3 ± 21.5 (117)
Nose	10.4 ± 1.4 (14)	84.4 ± 15 (18)	—
Cheek	9 ± 1.1 (13)	58.7 ± 9.7 (16)	—
Chest	9.1 ± 1.2 (14)	54.3 ± 5.9 (11)	22.6 ± 12.9 (57)
Back	9.5 ± 1.3 (14)	59.9 ± 4.5 (8)	27.5 ± 7.2 (26)
Forearm (posterior)	12.7 ± 3.2 (25)	70.7 ± 12.8 (18)	7 ± 10.1 (144)
Hand (back)	29.5 ± 5.7 (19)	98.9 ± 15.6 (16)	18.7 ± 22.8 (122)

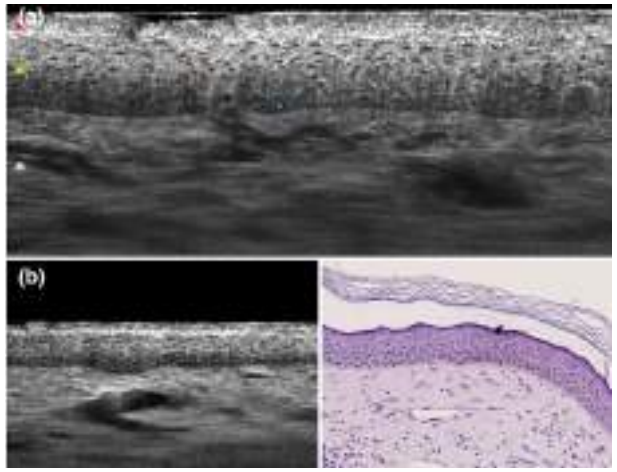

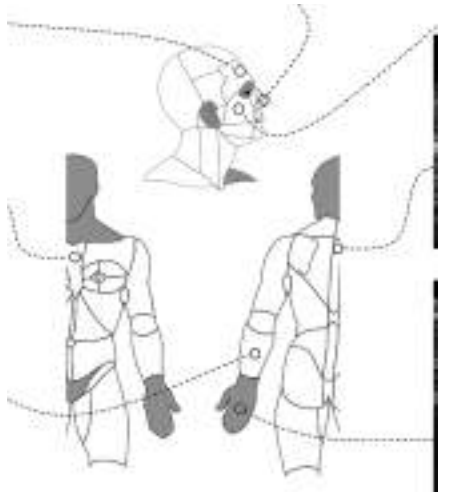

Monnier J, Tognetti L, Miyamoto M, Suppa M, Cinotti E, Fontaine M, Perez J, Orte Cano C, Yélamos O, Puig S, Dubois A, Rubegni P, Del Marmol V, Malvehy J, Perrot JL. In vivo characterization of healthy human skin with a novel, non-invasive imaging technique: line-field confocal optical coherence tomography. J Eur Acad Dermatol Venereol. 2020 Dec;34(12):2914-2921

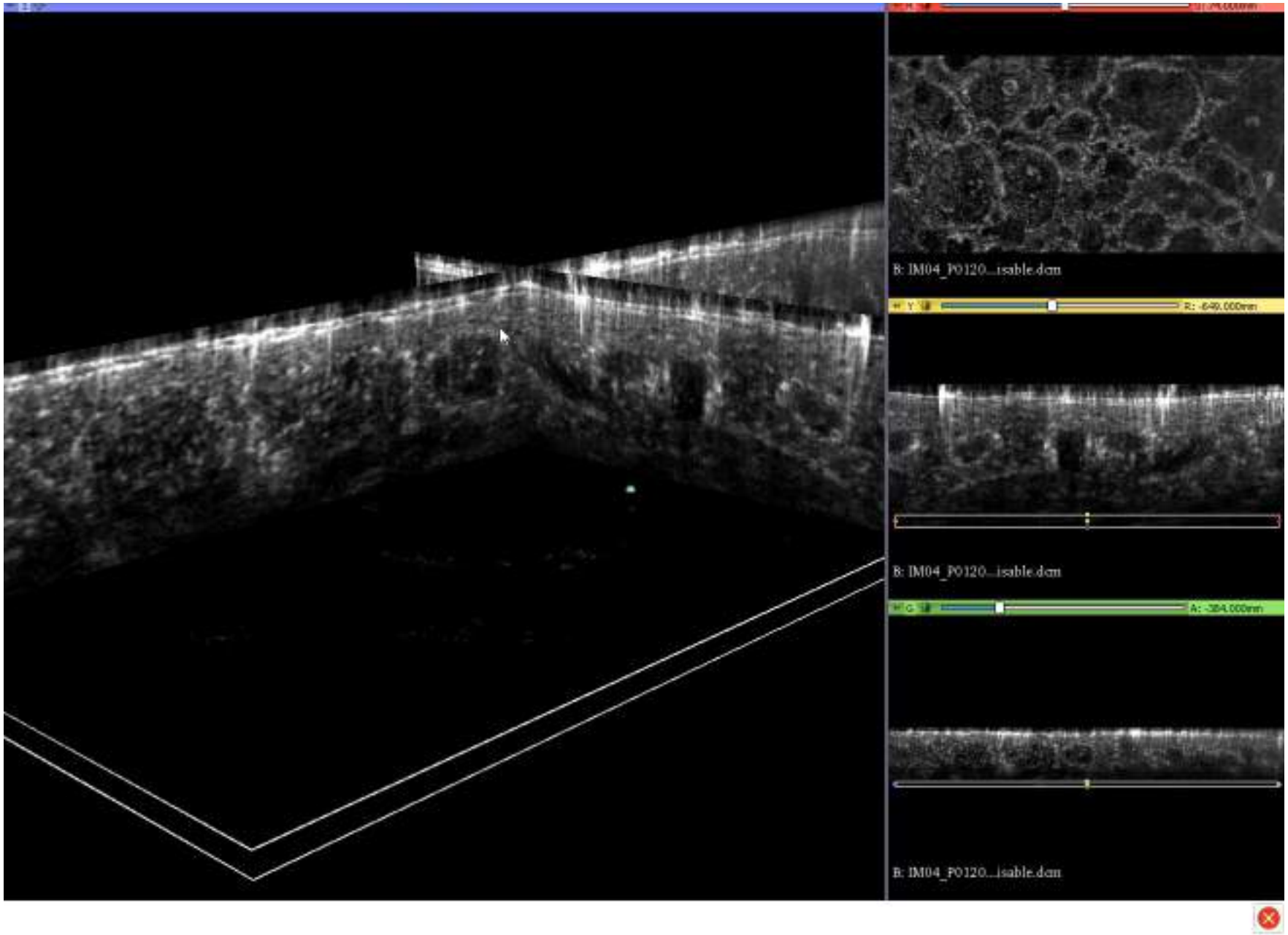
B: IM04_P0120...isable.dcm
B: IM04_P0120...isable.dcm
B: IM04_P0120...isable.dcm

movie

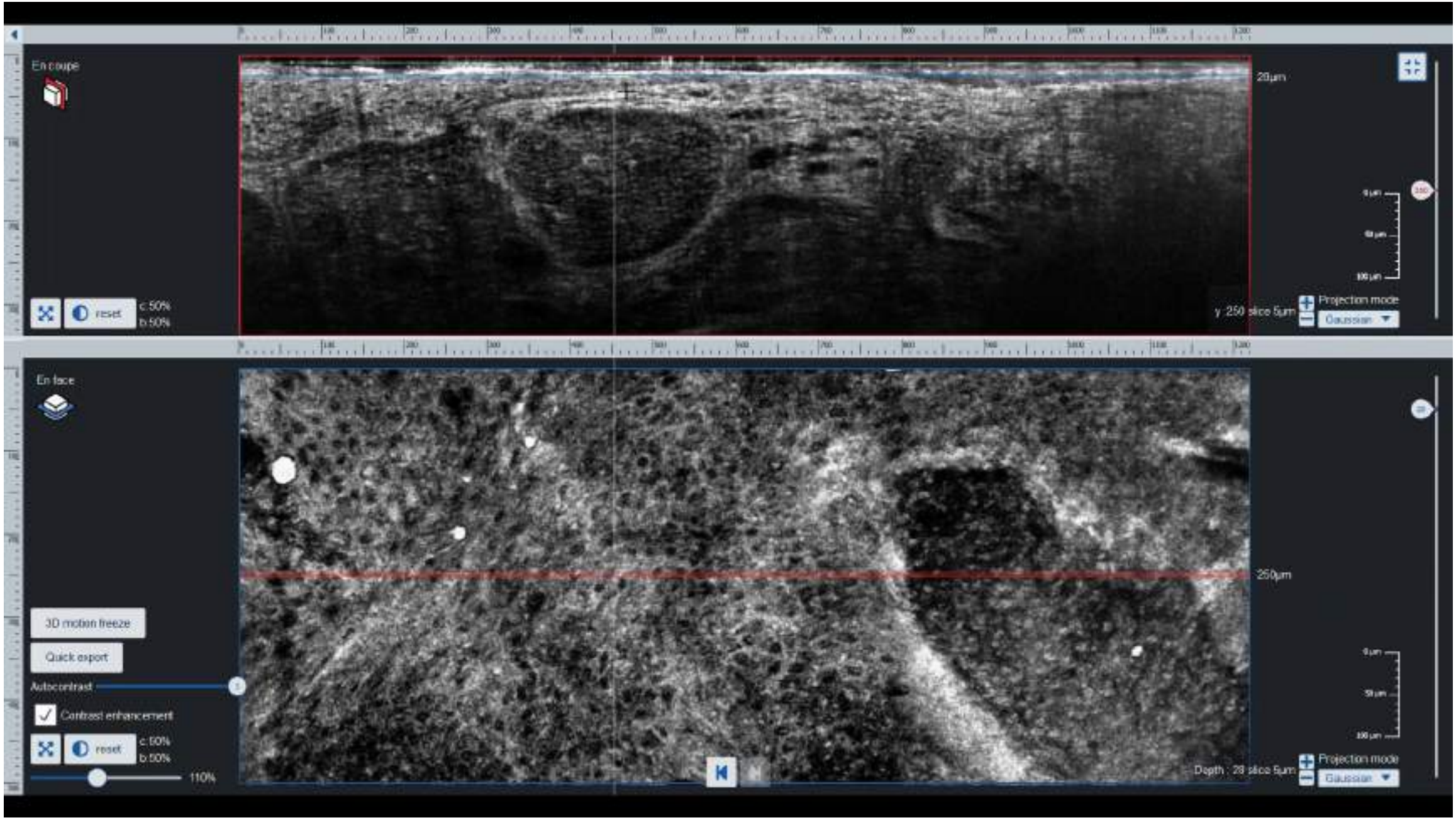
En coupe
reset
c: 50%
b: 50%
y: 250 slice 5µm
Projection mode
Gaussian
En face
3D motion freeze
Quick export
Autocontrast
Contrast enhancement
reset
c: 50%
b: 50%
110%
Depth : 28 slice 5µm
Projection mode
Gaussian

movie

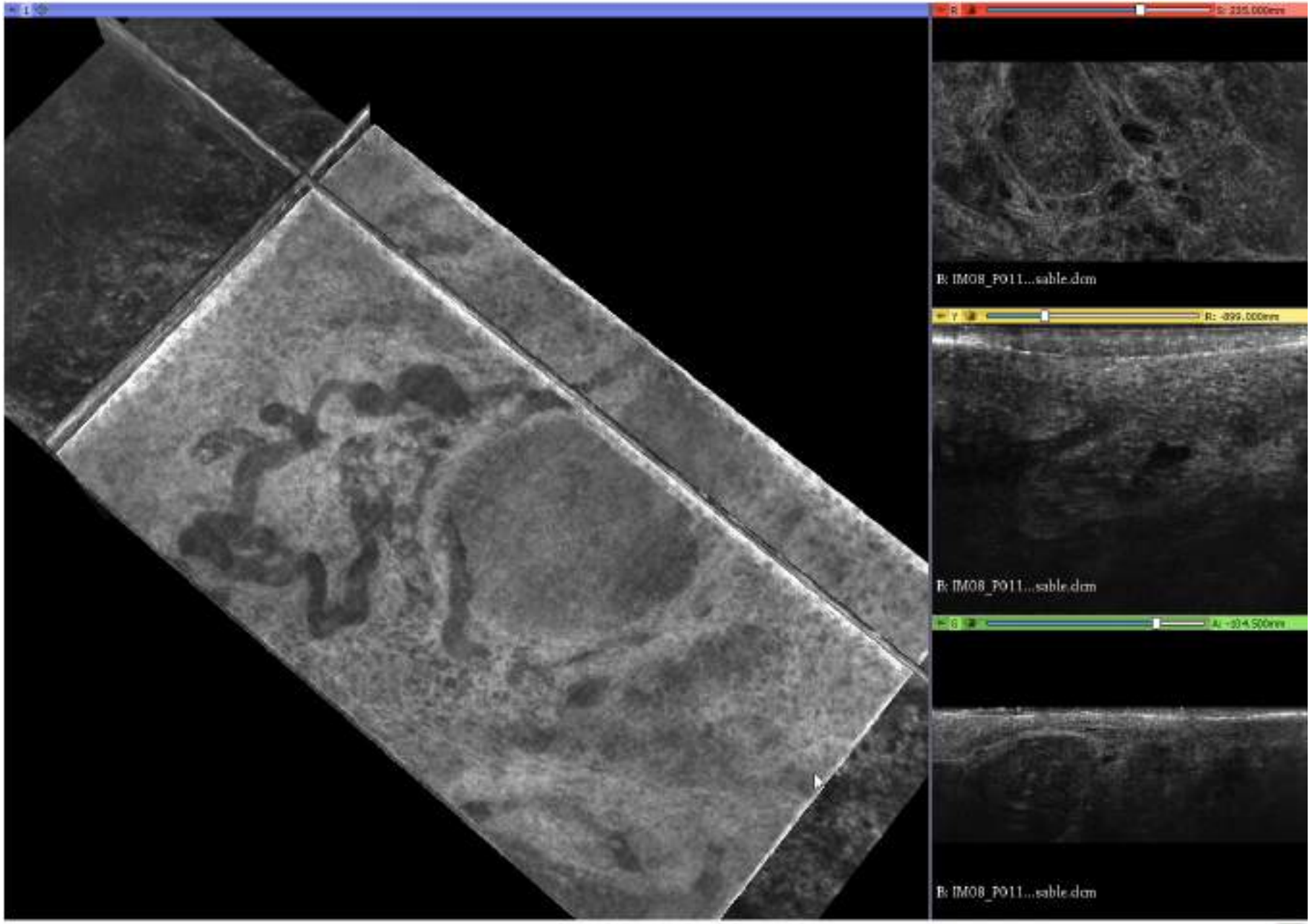
B: IM08_P011...sable.dcm
B: IM08_P011...sable.dcm
B: IM08_P011...sable.dcm

movie

P115, SCC

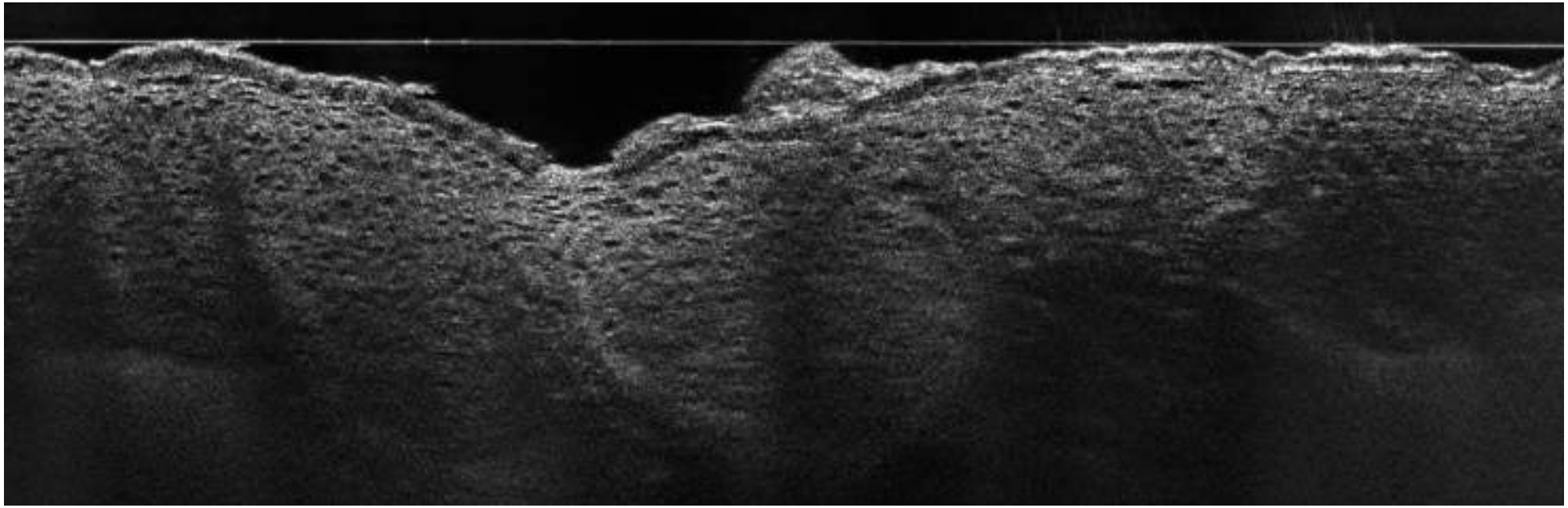

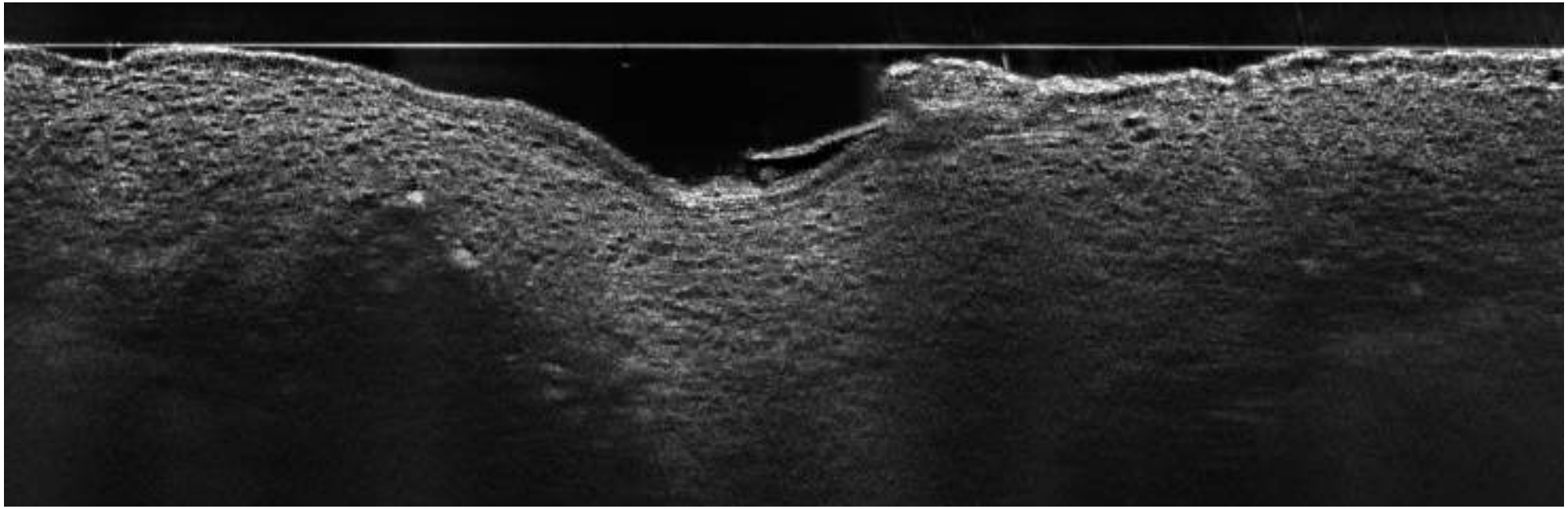

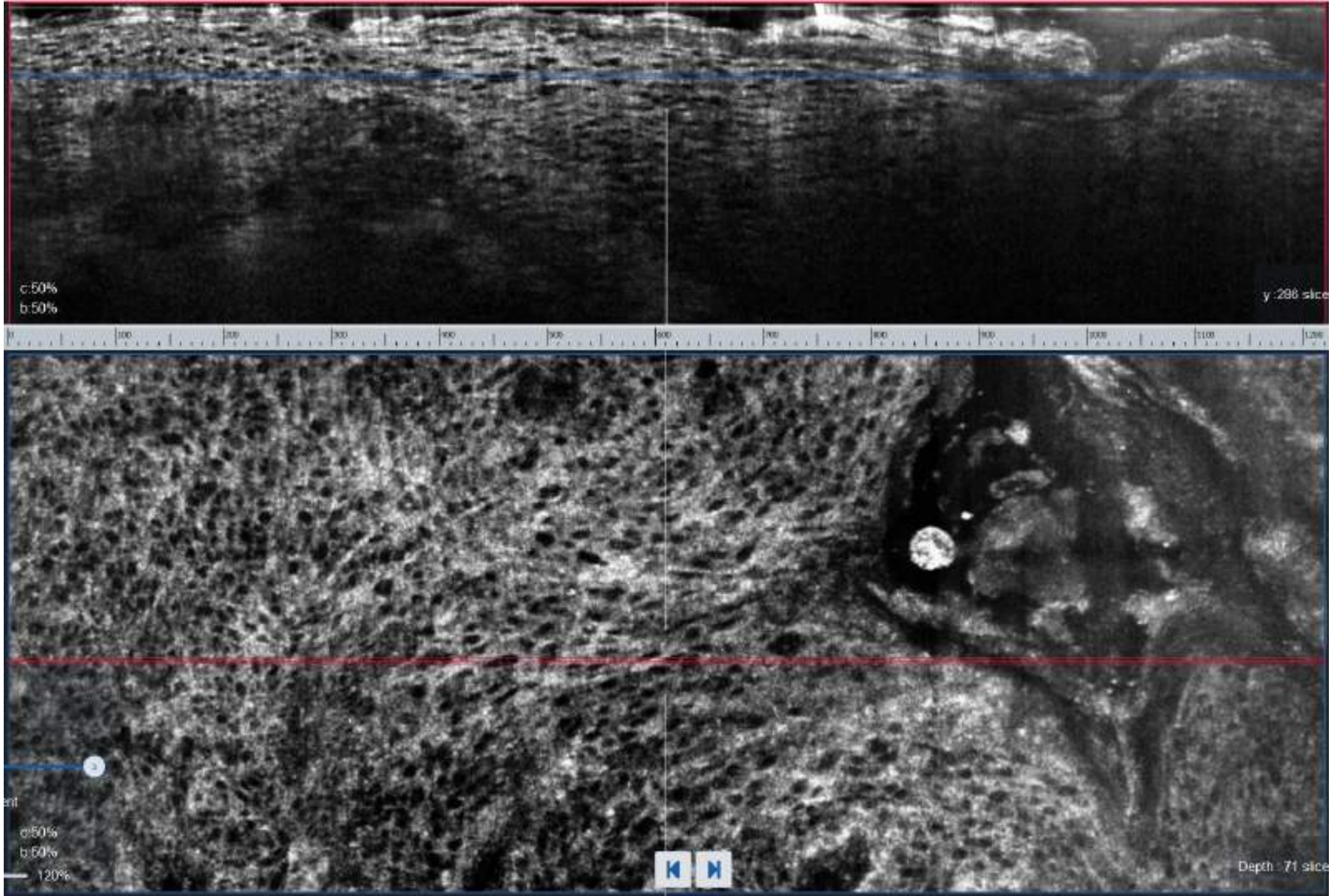
c:50%
b:50%
y :286 slice
c:50%
b:60%
120%
Depth : 71 slice

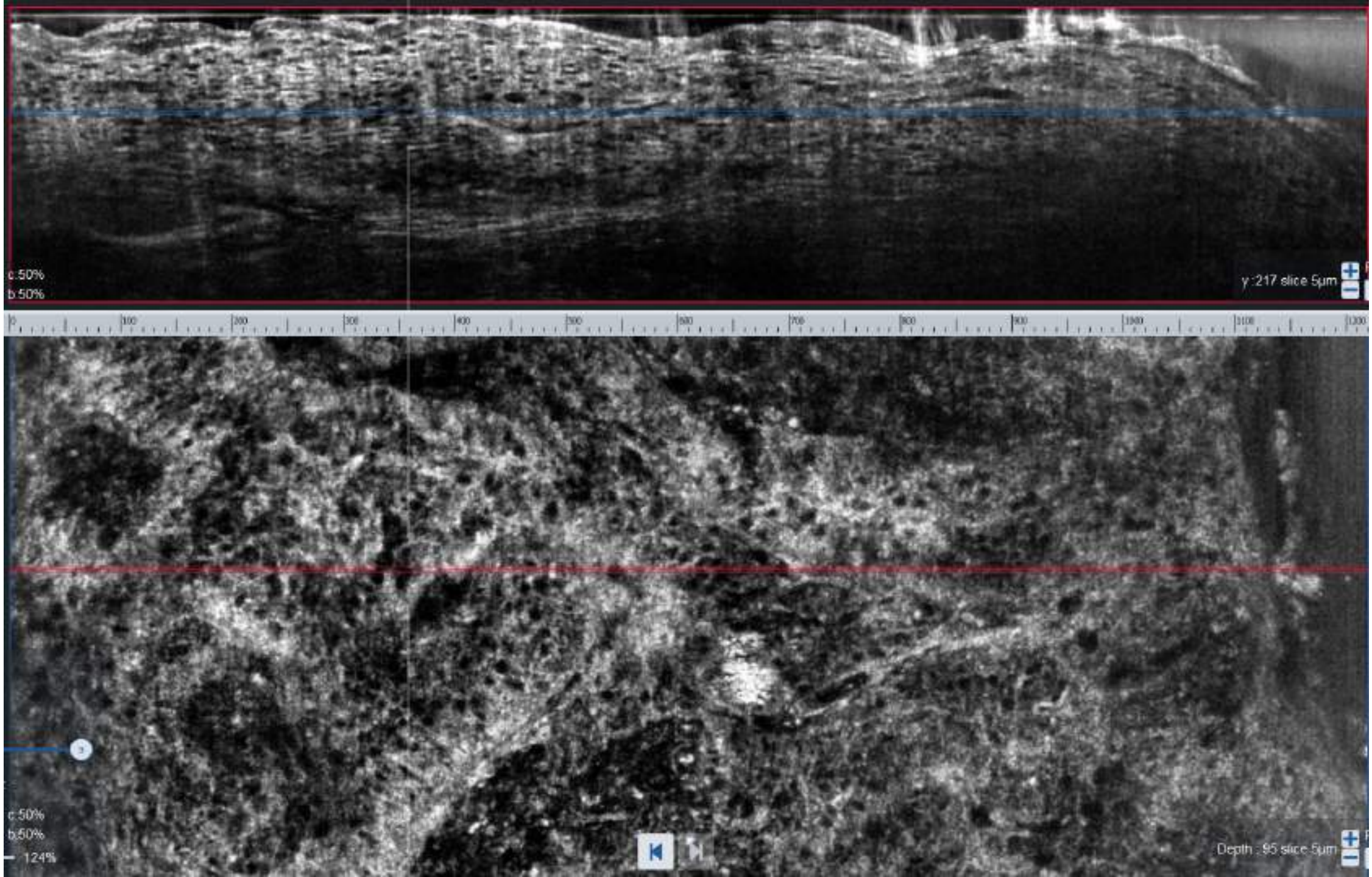
c:50%
b:50%
y :217 slice 5µm
c:50%
b:50%
124%
Depth : 95 slice 5µm

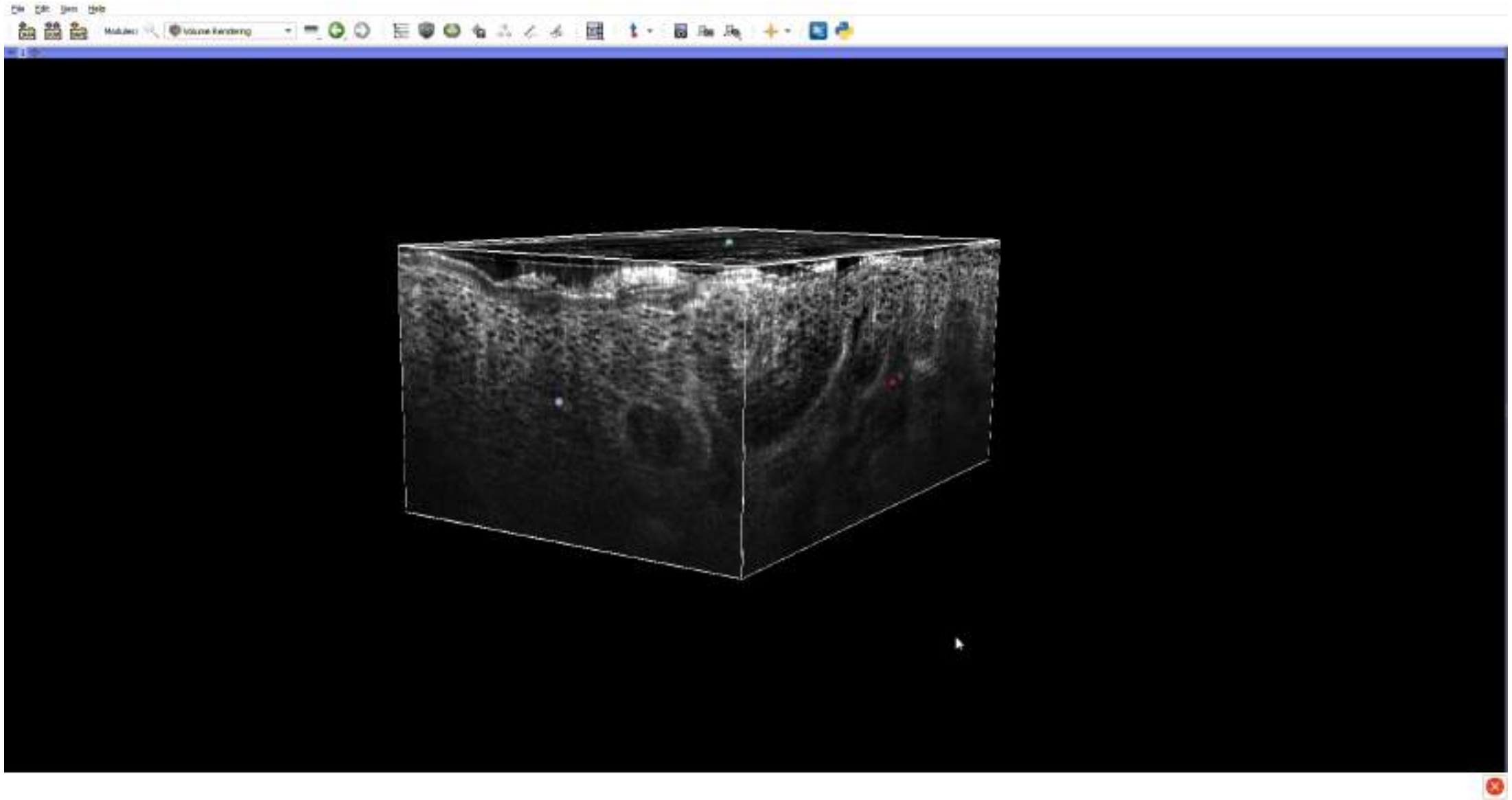

movie

Line-field confocal optical coherence tomography of basal cell carcinoma: a descriptive study

Table 1 Description of LC-OCT criteria for basal cell carcinoma (based on literature review and expert opinion)

LC-OCT criteria	Description	Interpretation
Lobule	Structure with variable shape, size and location within the dermis, characterized by a grey core usually surrounded by a darker rim	Aggregates of basaloid cells growing into the dermis (BCC tumour islands)
Macrolobules	Much larger than the size of epidermis (>100 μm)	Large aggregates of basaloid cells (>100 μm)
Microlobules	Equal or smaller than the size of epidermis (<100 μm)	Small aggregates of basaloid cells (<100 μm)
Millefeuille pattern	Specific LC-OCT pattern characterized by a grey, laminated structure at the core of the BCC lobule, orientated along the horizontal plane. It resembles the pattern seen in the eponymous French delicacy *millefeuille*	Dense cellularity orientated along the same axis within the tumour island, composed of basaloid cells, immune cells, apoptotic bodies and mitotic figures
Clefting	Dark rim surrounding the core of the lobule	Peritumoral mucin deposition
Bright rim	Outer rim surrounding the lobule characterized by a brighter colour than the stroma	Compression/alteration of the collagen fibres of the stroma by the tumour island (mass effect and tumour- stroma interaction)
Triad of colours	The simultaneous presence of inner lamination, middle clefting and outer bright rim gives rise to a cockade aspect, characterized by three colours (grey, black and white, respectively)	Classic appearance of a BCC tumour island, especially seen in nBCC
Lobule location		
Separated from epidermis	Absence of lobule connection with the epidermis	Tumour island not connected to the epidermis: it points to other subtypes than sBCC
Connected to epidermis	Presence of lobule connection with the epidermis	Tumour island connected to the epidermis: it points to sBCC subtype
Lobule morphology	Various morphologies can be encountered: *round*, *elongated/ovoid*, *hemispheric* (usually leaning towards the epidermis), *branched* (lobule dividing into one or more subdivisions with progressive loss of contour definition) and *polymorphic* (simultaneous presence of two or more morphologies)	Various morphologies of the tumour islands may point to particular BCC subtypes (e.g. hemispheric morphology suggests sBCC; branched morphology suggests iBCC)
Blood vessels	Well-defined, hypo-reflective structures of various shape/size localized within the dermis and especially next to lobules. In the LC-OCT *in vivo* acquisition modality and videos, hyper-reflective elements can be seen flowing within them	Dermal blood vessels, particularly prominent when next to tumour islands (neo-angiogenesis); blood cell flow can be visualized within them
Stroma		
Stretching	The dermis surrounding the lobules appears stretched, i.e. polarized in one direction	Distortion of the collagen/elastic fibres of the stroma due to the presence of tumour islands (mass effect and tumour-stroma interaction). It is more common in BCC subtypes other than sBCC
Brightness	The dermis surrounding the lobules appears whiter (brighter) than the overlying epidermis	Increased reflectivity of the stroma due to the presence of tumour islands (mass effect and tumour–stroma interaction). It is more common in BCC subtypes other than sBCC
Epidermal changes		
Parakeratosis	Dark little roundish structures in the upper layer of the epidermis	Nucleated keratinocytes in the stratum corneum
Disorganized epidermis	Variability of size and shape of the keratinocytes' nuclei within a particular layer of the epidermis	Pleomorphism in the epidermis
Disrupted dermal-epidermal junction	Loss of a clear separation between the epidermis and the dermis	It may be related to the presence of hemispheric lobules leaning towards the epidermis or the loss of its visibility due to ulceration, crusts or artefacts
Bright cells within epidermis/lobules	Hyper-reflective structures within the epidermis and/or within the lobules. They can have various shape/size: small, large or dendritic (tree-like shape or spindle shape)	Immunologically competent skin cells (Langerhans cells and granulocytes) and activated melanocytes in pigmented BCCs
Other criteria		
Erosion/Ulceration	Partial/complete loss of continuity of the epidermis (without/with involvement of the DEJ)	Partial/complete loss of the epidermis (without/with involvement of the basal membrane)
Crust	Accumulation of hyper- and hypo-reflective structures overlying the epidermis	Dried material (sebum, pus, blood, serum) usually mixed with epithelial debris, at the surface of the lesion

Table 2 Characteristics of the basal cell carcinomas included in the study

	Overall	Head/neck	Trunk	Upper extremities	Lower extremities
Pure BCC subtypes					
Superficial	19 (21.4)	7 (13.7)	5 (23.8)	4 (80.0)	3 (37.5)
Nodular	31 (34.8)	17 (33.3)	8 (38.1)	0 (0)	2 (25.0)
Infiltrative	16 (18.0)	9 (17.7)	5 (23.8)	0 (0)	2 (25.0)
Mixed BCC subtypes					
Superficial and infiltrative	8 (9.0)	6 (11.8)	2 (9.5)	0 (0)	0 (0)
Superficial and nodular	5 (5.6)	4 (7.8)	1 (4.8)	0 (0)	0 (0)
Nodular and infiltrative	7 (7.9)	6 (11.8)	0 (0)	1 (20.0)	0 (0)
Superficial, nodular and infiltrative	1 (1.1)	1 (2.0)	0 (0)	0 (0)	0 (0)
Metatypical	1 (1.1)	0 (0)	0 (0)	0 (0)	1 (12.5)
Fibroepithelioma of pinkus	1 (1.1)	1 (2.0)	0 (0)	0 (0)	0 (0)
Total	**89**	**51**	**21**	**5**	**8**

N (%) displayed in each box. Numbers do not always add up to the total due to missing values.
BCC, basal cell carcinoma.

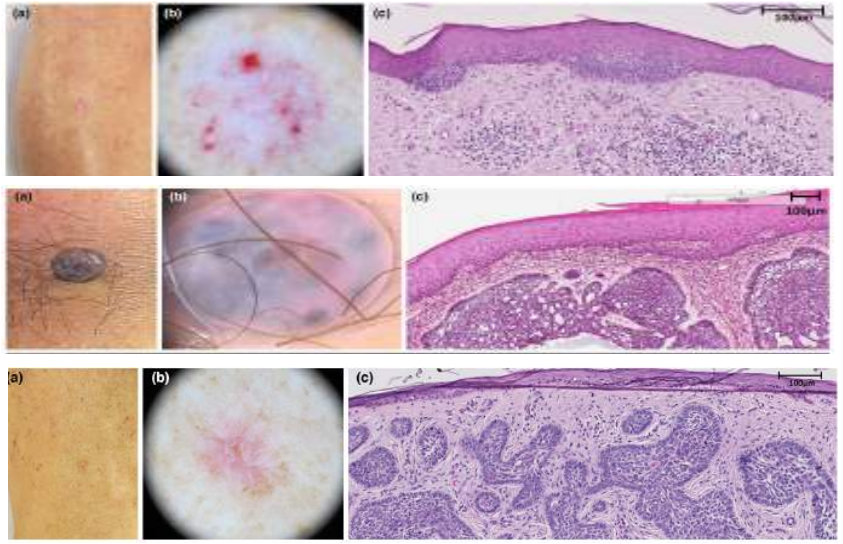

Suppa M, Fontaine M, Dejonckheere G, Cinotti E, Yélamos O, Diet G, Tognetti L, Miyamoto M, Orte Cano C, Perez-Anker J, Panagiotou V, Trepant AL, Monnier J, Berot V, Puig S, Rubegni P, Malvehy J, Perrot JL, Del Marmol V. Line-field confocal optical coherence tomography of basal cell carcinoma: a descriptive study. J Eur Acad Dermatol Venereol. 2020 Dec 7.

Line-field confocal optical coherence tomography of basal cell carcinoma: a descriptive study

Table 3 Distribution of LC-OCT criteria overall and according to BCC subtype

	A. Overall	B. According to BCC subtype			*P*-value
	(*n* = 89)	sBCC (*n* = 19)	nBCC (*n* = 31)	iBCC (*n* = 16)	
Lobule	88 (98.9)	19 (100)	30 (96.8)	16 (100)	0.56
Lobule size					
Macrolobules	73 (82.0)	9 (47.4)	29 (93.5)	14 (87.5)	**<0.001**
Microlobules	49 (55.1)	14 (73.7)	12 (38.7)	10 (62.5)	**0.04**
Lobule composition					
Lamination	75 (84.3)	14 (73.7)	29 (93.5)	14 (87.5)	0.14
Clefting	82 (92.1)	18 (94.7)	29 (93.5)	15 (93.8)	0.99
Bright rim	66 (74.2)	9 (47.4)	27 (87.1)	14 (87.5)	**0.003**
Triad of colours	56 (62.9)	5 (26.3)	24 (77.4)	12 (75.0)	**0.001**
Lobule location					
Separated from epidermis	68 (76.4)	7 (36.8)	28 (90.3)	15 (93.8)	**<0.001**
Connected to epidermis	57 (64.0)	19 (100.0)	15 (48.4)	10 (62.5)	**0.001**
Lobule morphology					
Round	42 (47.2)	5 (26.3)	16 (51.6)	10 (62.5)	0.08
Elongated	56 (62.9)	6 (31.6)	24 (77.4)	11 (68.8)	**0.004**
Hemispheric	23 (25.8)	12 (63.2)	5 (16.1)	1 (6.3)	**<0.001**
Branched	25 (28.1)	3 (15.8)	9 (29.0)	9 (56.3)	**0.03**
Polymorphic	11 (12.4)	2 (10.5)	4 (12.9)	2 (12.5)	0.97
Blood vessels	84 (94.4)	16 (84.2)	31 (100)	16 (100)	0.02
Stroma involvement					
Stretching	68 (76.4)	8 (42.1)	27 (87.1)	14 (87.5)	**0.001**
Brightness	41 (46.1)	4 (21.1)	17 (54.8)	9 (56.3)	**0.04**
Epidermal changes					
Parakeratosis	17 (19.1)	1 (5.3)	9 (29.0)	1 (6.3)	**0.04**
Disorganized epidermis	17 (19.1)	4 (21.1)	7 (22.6)	4 (25.0)	0.96
Disrupted DEJ	57 (64.0)	15 (78.9)	16 (51.6)	11 (68.8)	0.13
Bright cells within epidermis					
Small bright cell	86 (96.6)	19 (100.0)	30 (96.8)	15 (93.8)	0.56
Large bright cell	9 (10.1)	0 (0.0)	3 (9.7)	3 (18.8)	0.16
Dendritic bright cell	4 (4.5)	1 (5.3)	0 (0.0)	1 (6.3)	0.40
Bright cells within lobules					
Small bright cell	78 (87.6)	15 (78.9)	29 (93.5)	14 (87.5)	0.31
Large bright cell	21 (23.6)	1 (5.3)	12 (38.7)	5 (31.3)	**0.03**
Dendritic bright cell	9 (10.1)	0 (0.0)	6 (19.4)	2 (12.5)	0.13
Other					
Ulceration	24 (27.0)	2 (10.5)	11 (35.5)	4 (25.0)	0.15
Cysts	10 (11.2)	2 (10.5)	3 (9.7)	1 (6.3)	0.90
Crust	28 (31.5)	4 (21.1)	12 (38.7)	5 (31.3)	0.43

N (%) displayed in each box, unless otherwise stated.
P-values were calculated by means of Pearson's chi-squared test.
Significant findings are highlighted in bold.
DEJ, dermal–epidermal junction; iBCC, infiltrative basal cell carcinoma; nBCC, nodular basal cell carcinoma; sBCC, superficial basal cell carcinoma.

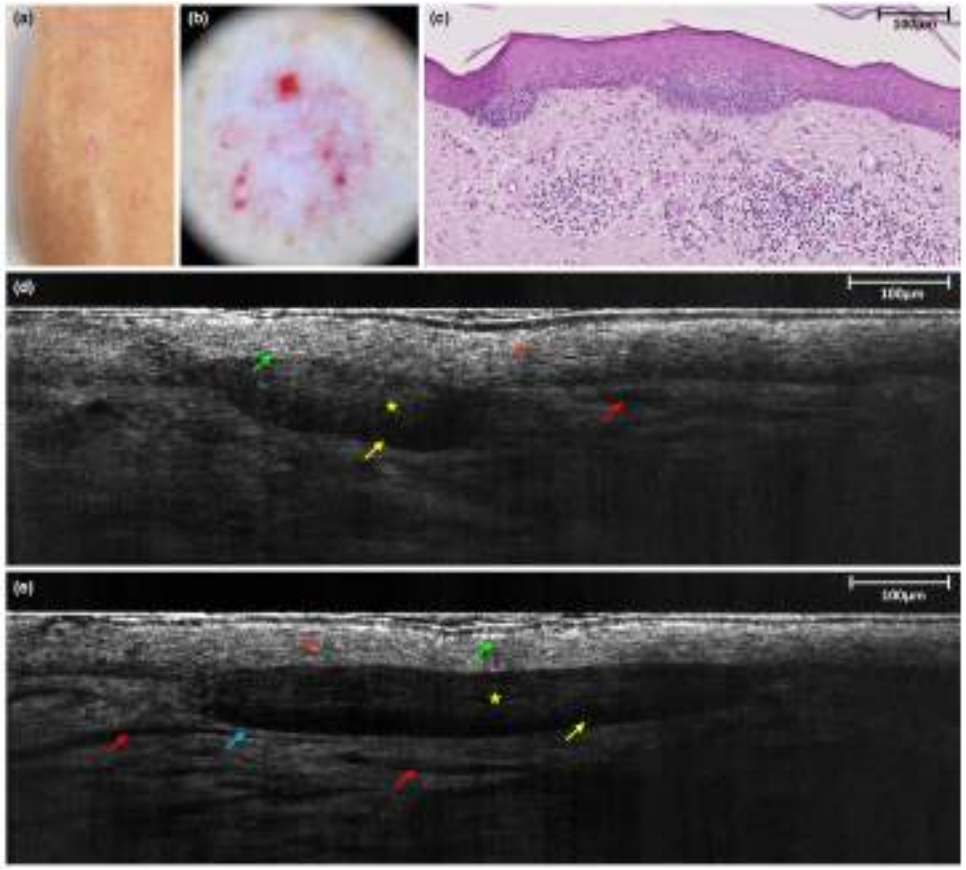

Suppa M, Fontaine M, Dejonckheere G, Cinotti E, Yélamos O, Diet G, Tognetti L, Miyamoto M, Orte Cano C, Perez-Anker J, Panagiotou V, Trepant AL, Monnier J, Berot V, Puig S, Rubegni P, Malvehy J, Perrot JL, Del Marmol V. Line-field confocal optical coherence tomography of basal cell carcinoma: a descriptive study. J Eur Acad Dermatol Venereol. 2020 Dec 7.

Line-field confocal optical coherence tomography of basal cell carcinoma: a descriptive study

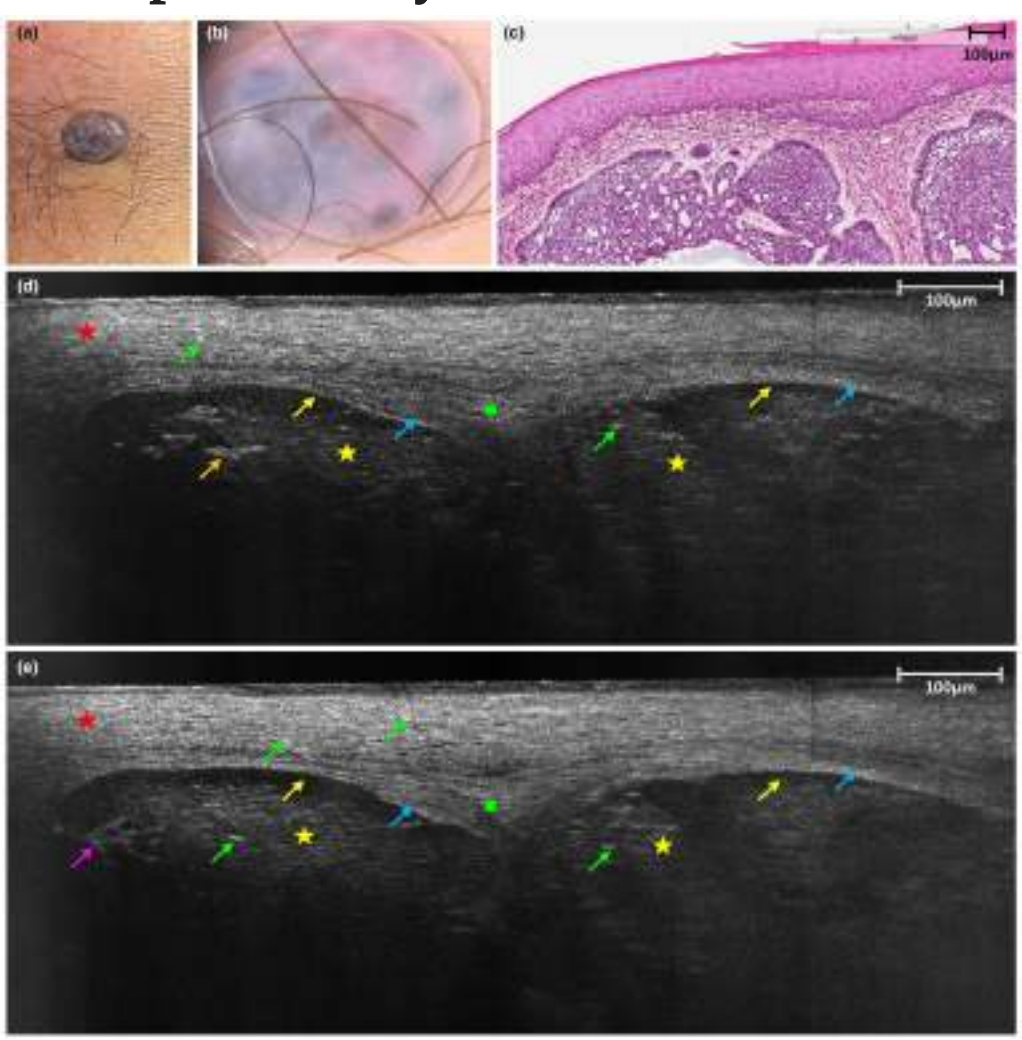

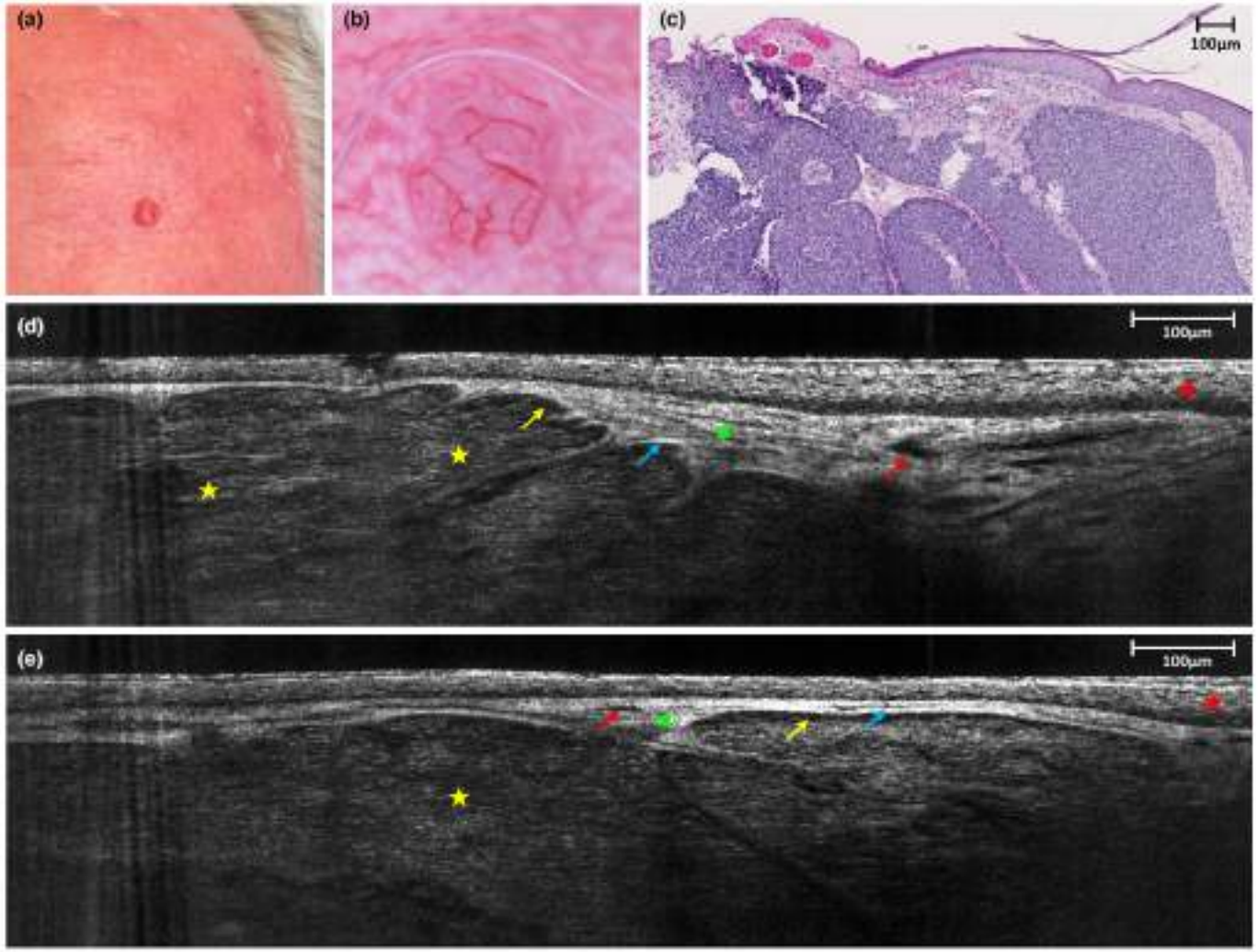

Suppa M, Fontaine M, Dejonckheere G, Cinotti E, Yélamos O, Diet G, Tognetti L, Miyamoto M, Orte Cano C, Perez-Anker J, Panagiotou V, Trepant AL, Monnier J, Berot V, Puig S, Rubegni P, Malvehy J, Perrot JL, Del Marmol V. Line-field confocal optical coherence tomography of basal cell carcinoma: a descriptive study. J Eur Acad Dermatol Venereol. 2020 Dec 7.

Line-field confocal optical coherence tomography of basal cell carcinoma: a descriptive study

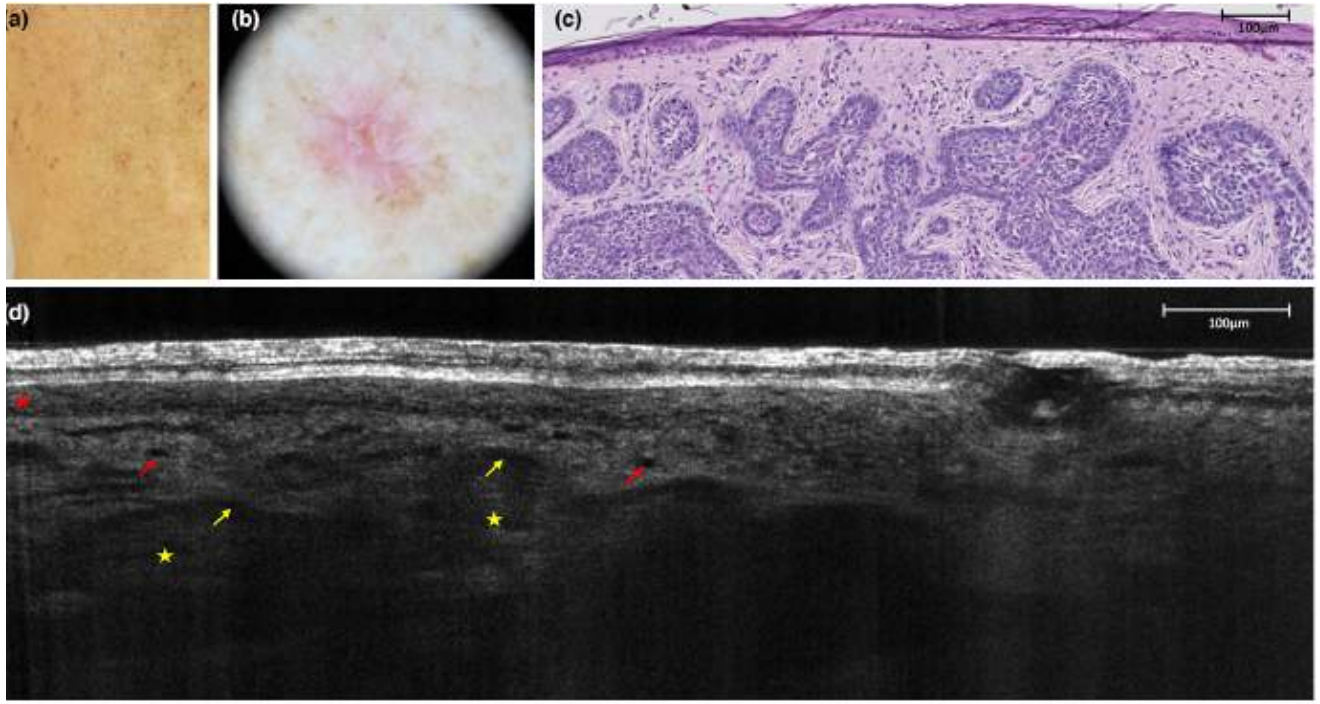

Table 4 Independent LC-OCT predictors of each BCC subtype

	OR (95% CI)	*P*-value
Superficial BCC		
Hemispheric lobule(s)	12.60 (2.10–75.57)	0.006
Lobule(s) separated from epidermis	0.19 (0.04–0.93)	0.04
Stretching of the stroma	0.09 (0.01–0.54)	0.008
Nodular BCC		
Macrolobule(s)	9.44 (1.66–53.65)	0.01
Lobule(s) connected to epidermis	0.16 (0.05–0.57)	0.005
Infiltrative BCC		
Branched lobule(s)	4.07 (1.25–13.27)	0.02

Suppa M, Fontaine M, Dejonckheere G, Cinotti E, Yélamos O, Diet G, Tognetti L, Miyamoto M, Orte Cano C, Perez-Anker J, Panagiotou V, Trepant AL, Monnier J, Berot V, Puig S, Rubegni P, Malvehy J, Perrot JL, Del Marmol V. Line-field confocal optical coherence tomography of basal cell carcinoma: a descriptive study. J Eur Acad Dermatol Venereol. 2020 Dec 7.

P119, IM6

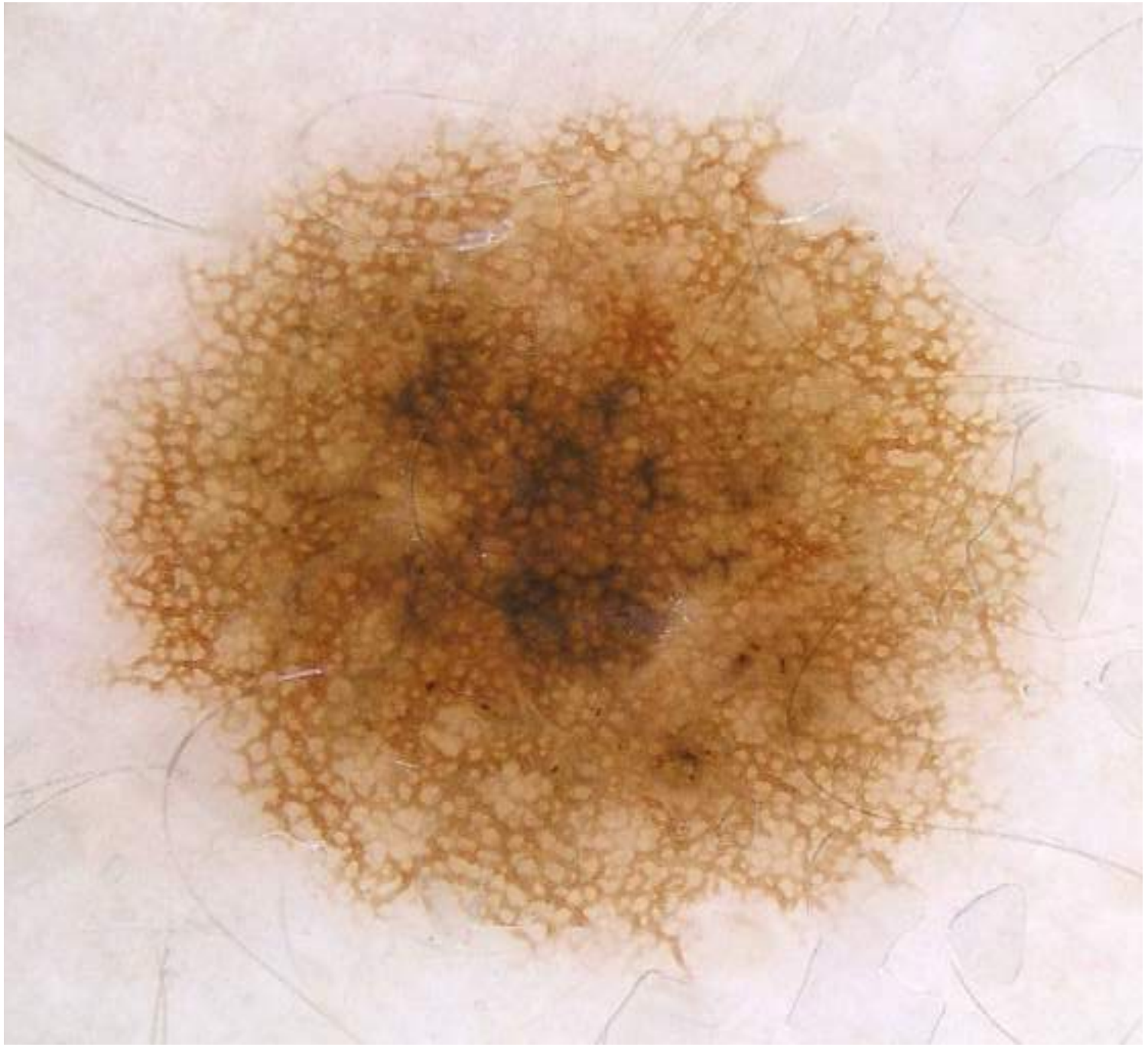

P119, IM6

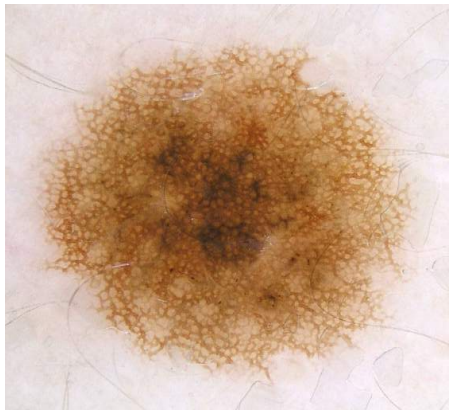

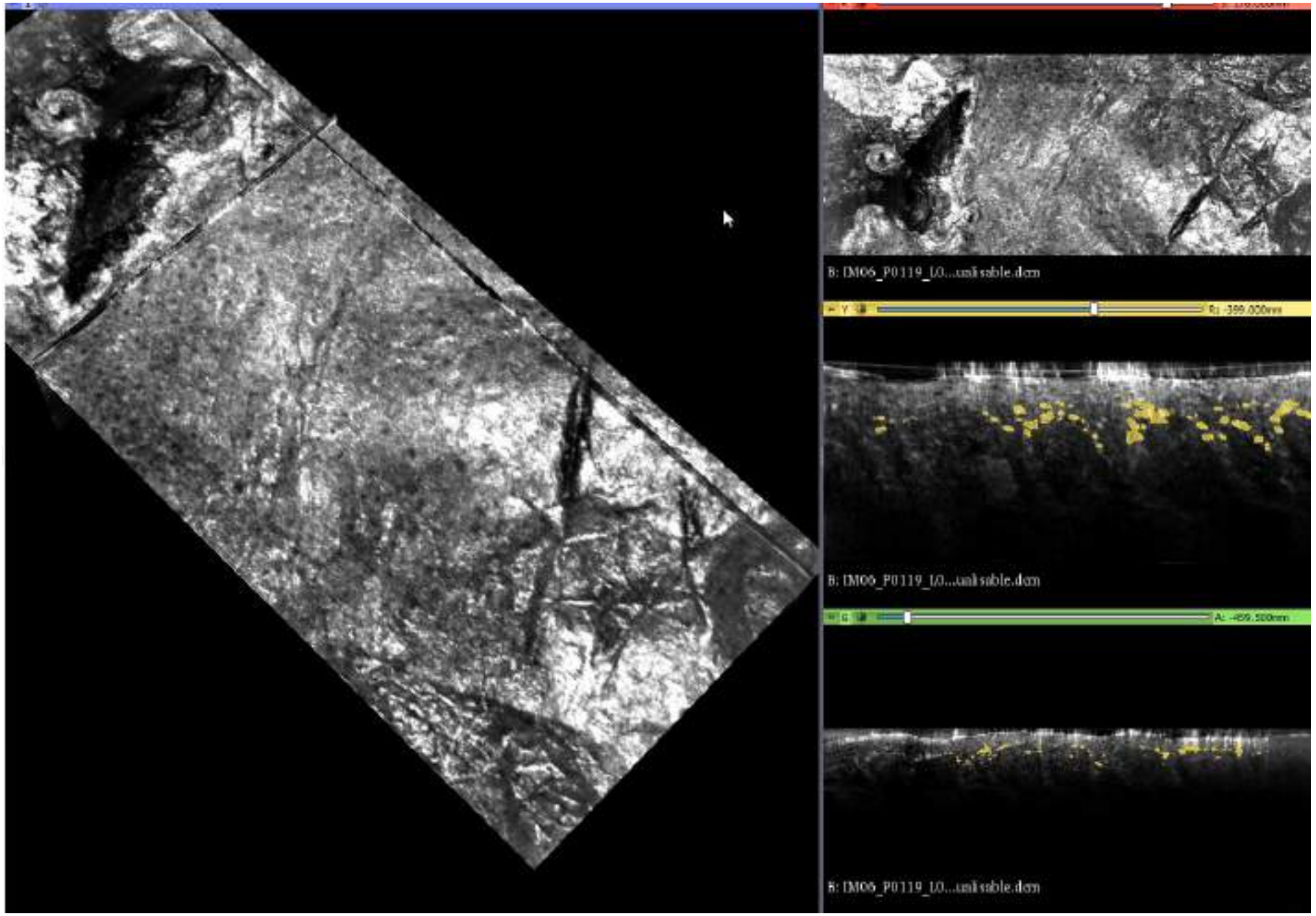

movie

P116, L1

P116, L1

P116, L1

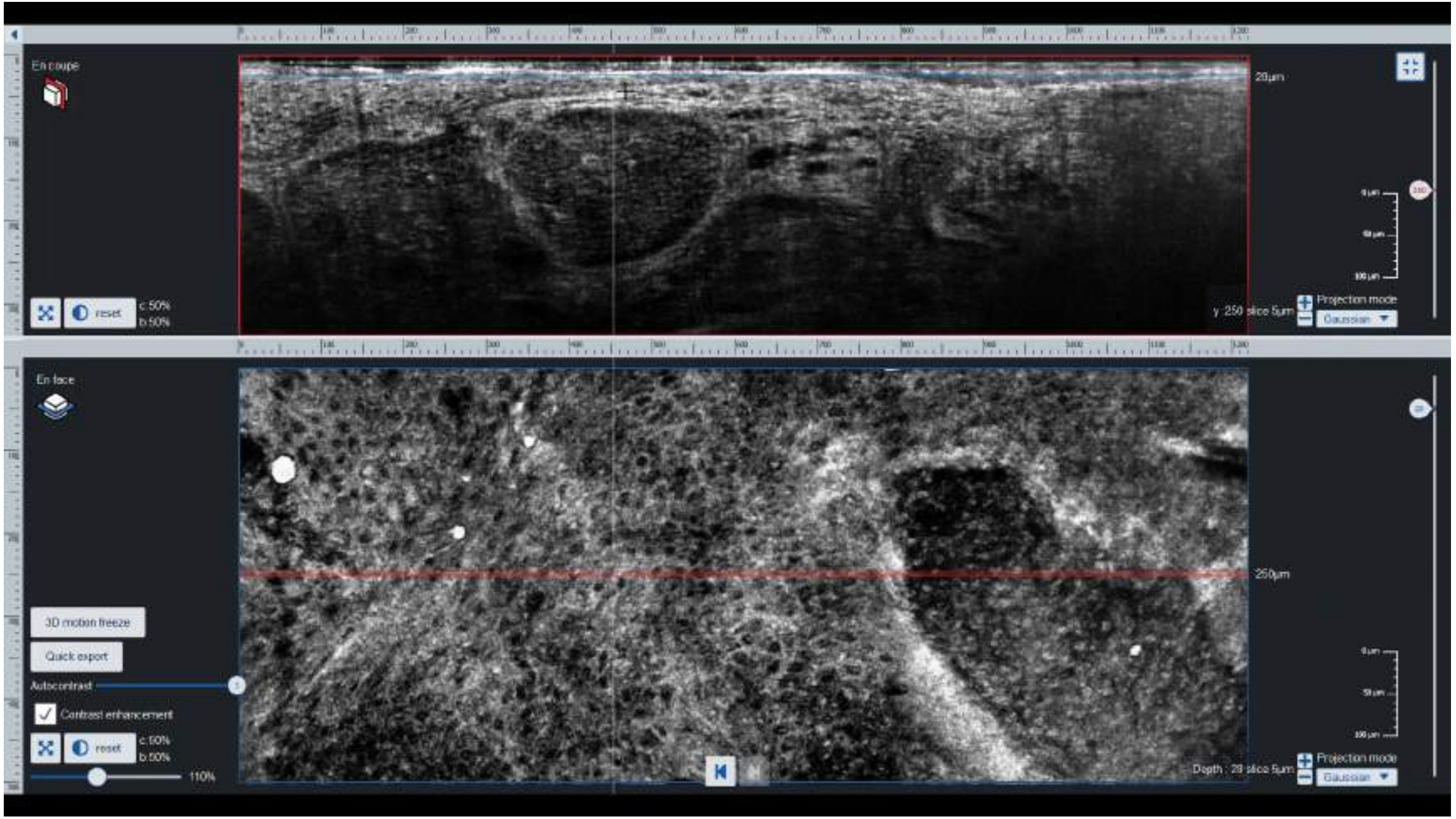
En coupe
reset
c: 50%
b: 50%
20µm
y: 250 slice 5µm
Projection mode
Gaussian
En face
3D motion freeze
Quick export
Autocontrast
Contrast enhancement
reset
c: 50%
b: 50%
110%
250µm
Depth : 28 slice 5µm
Projection mode
Gaussian

movie

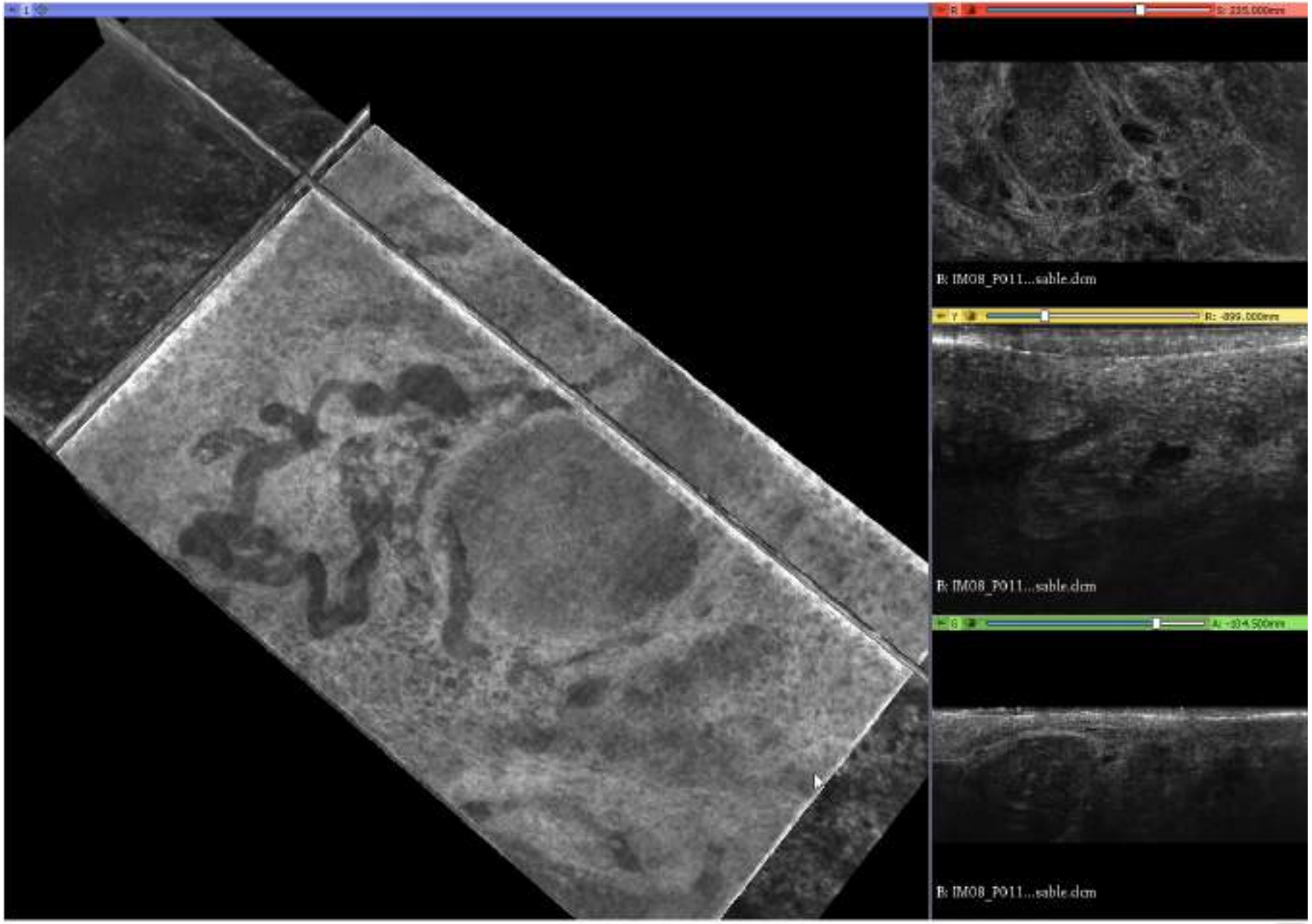
B: IM08_P011...sable.dcm
B: IM08_P011...sable.dcm
B: IM08_P011...sable.dcm

movie

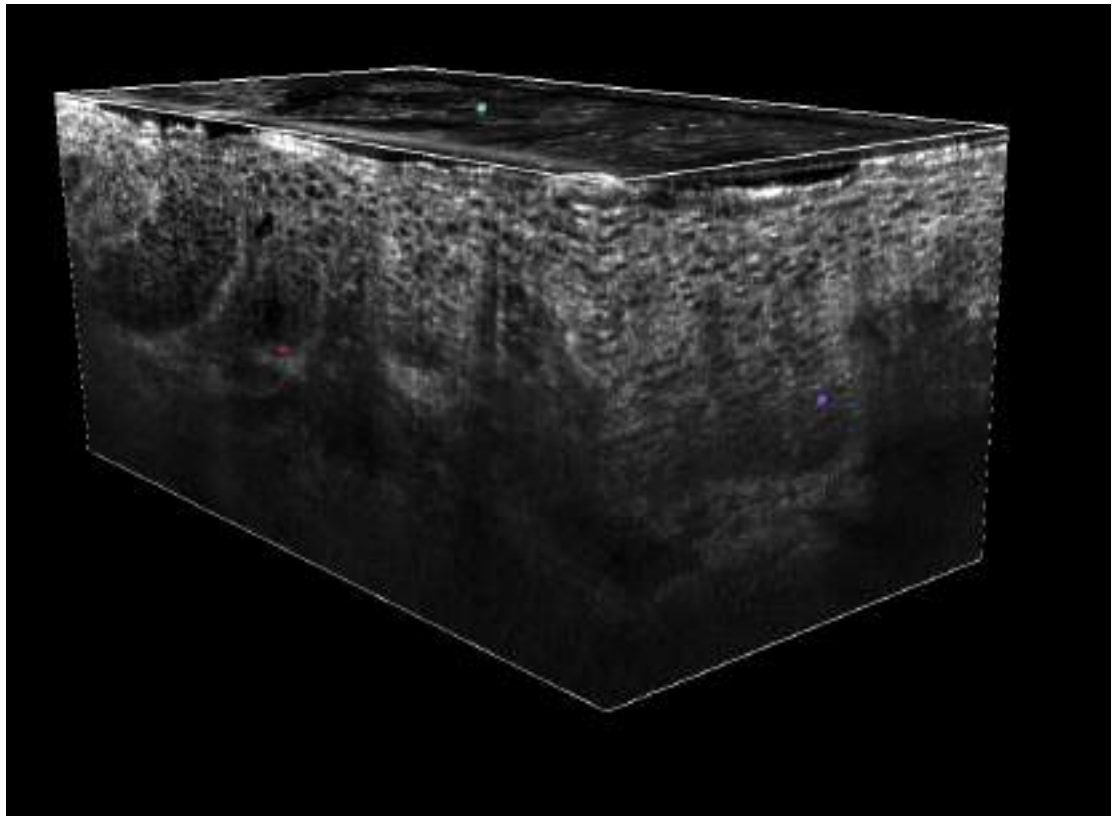

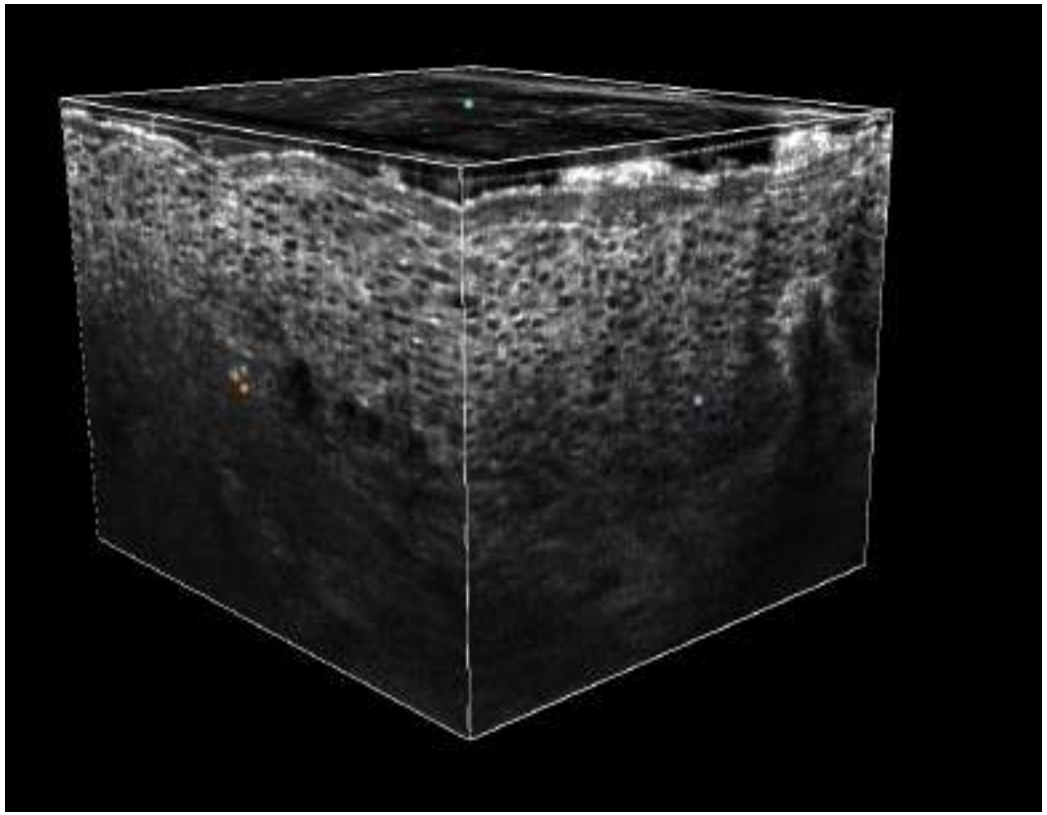

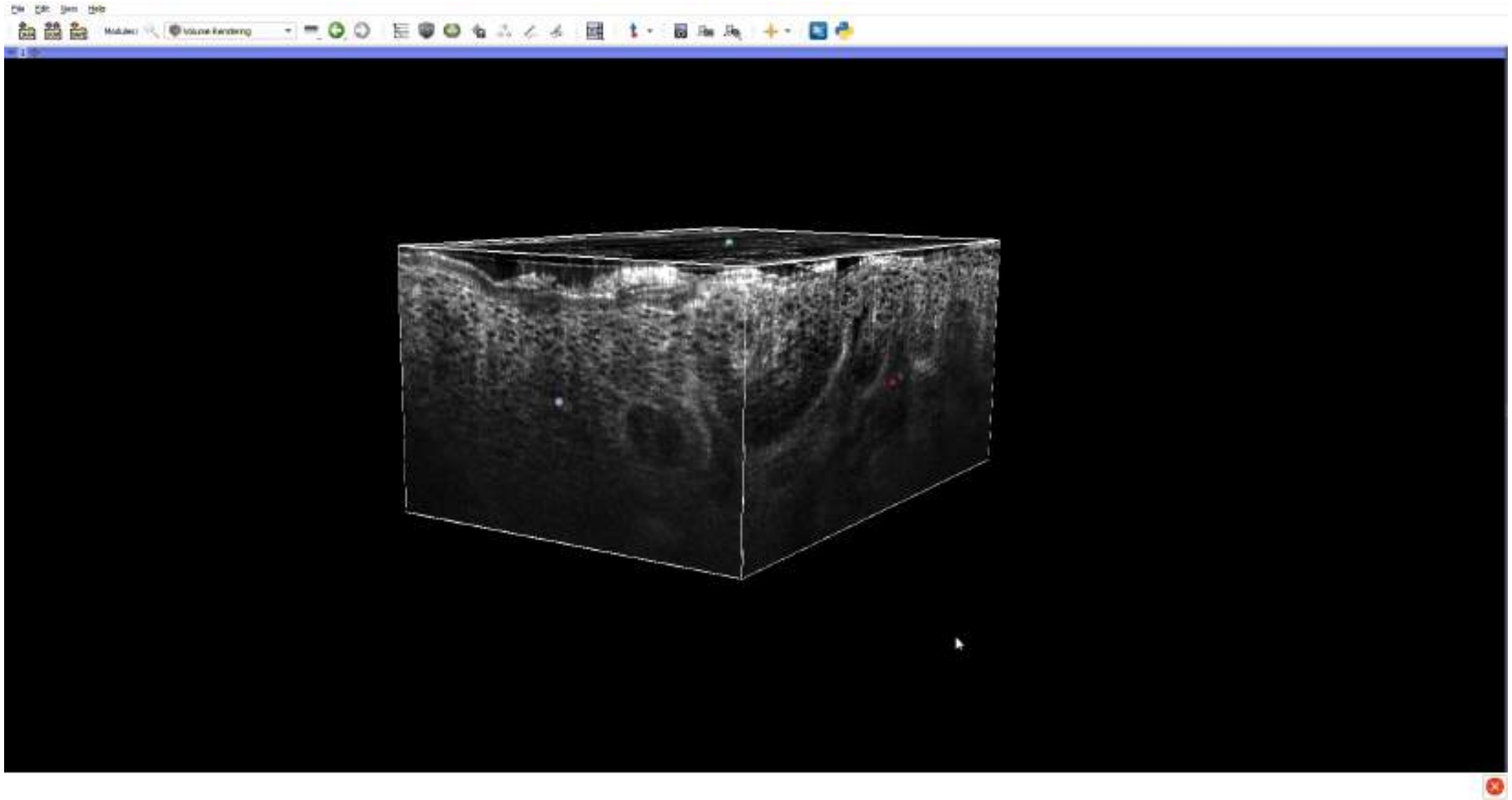

movie

P115, SCC

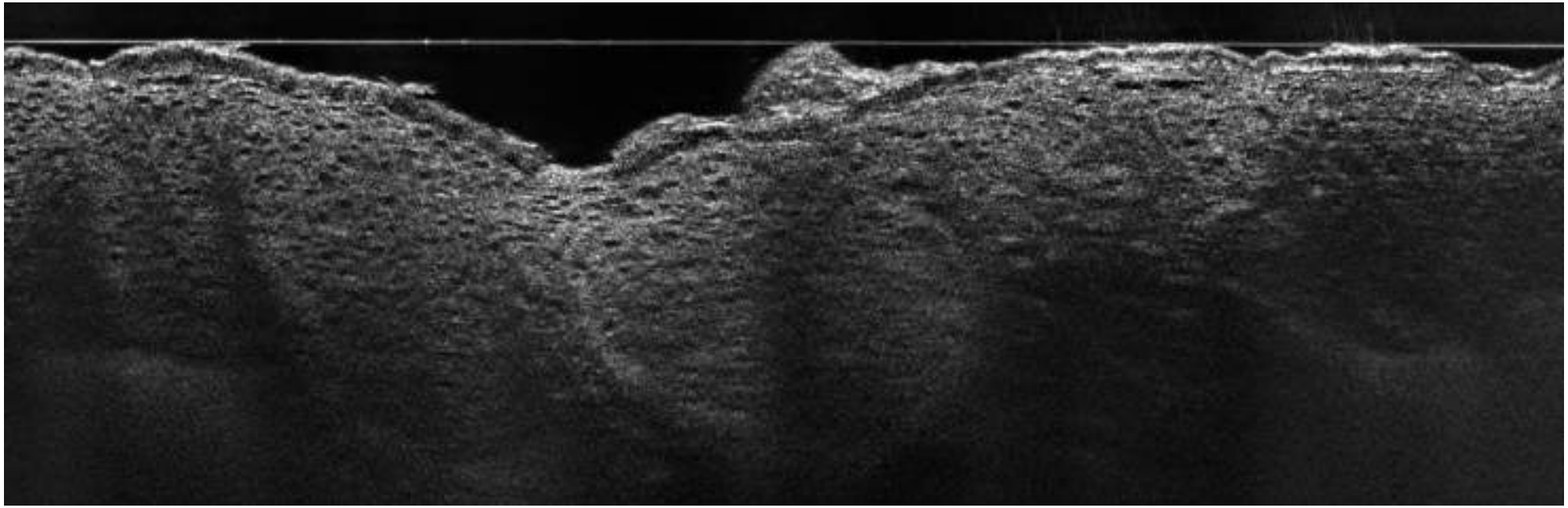

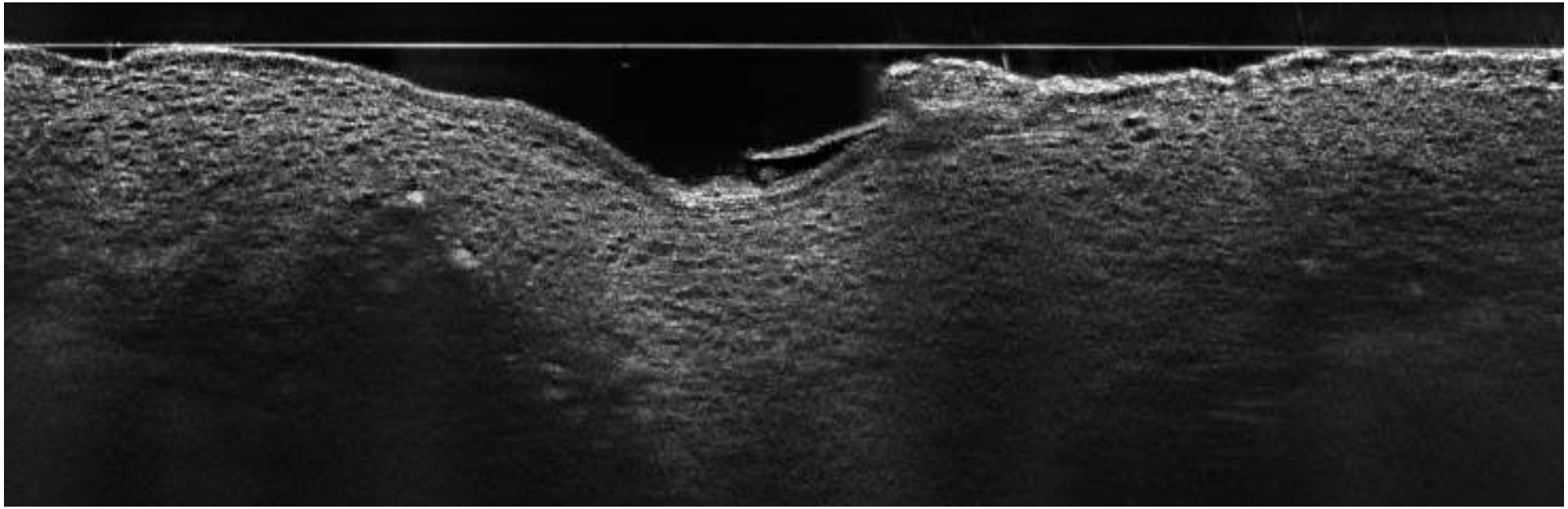

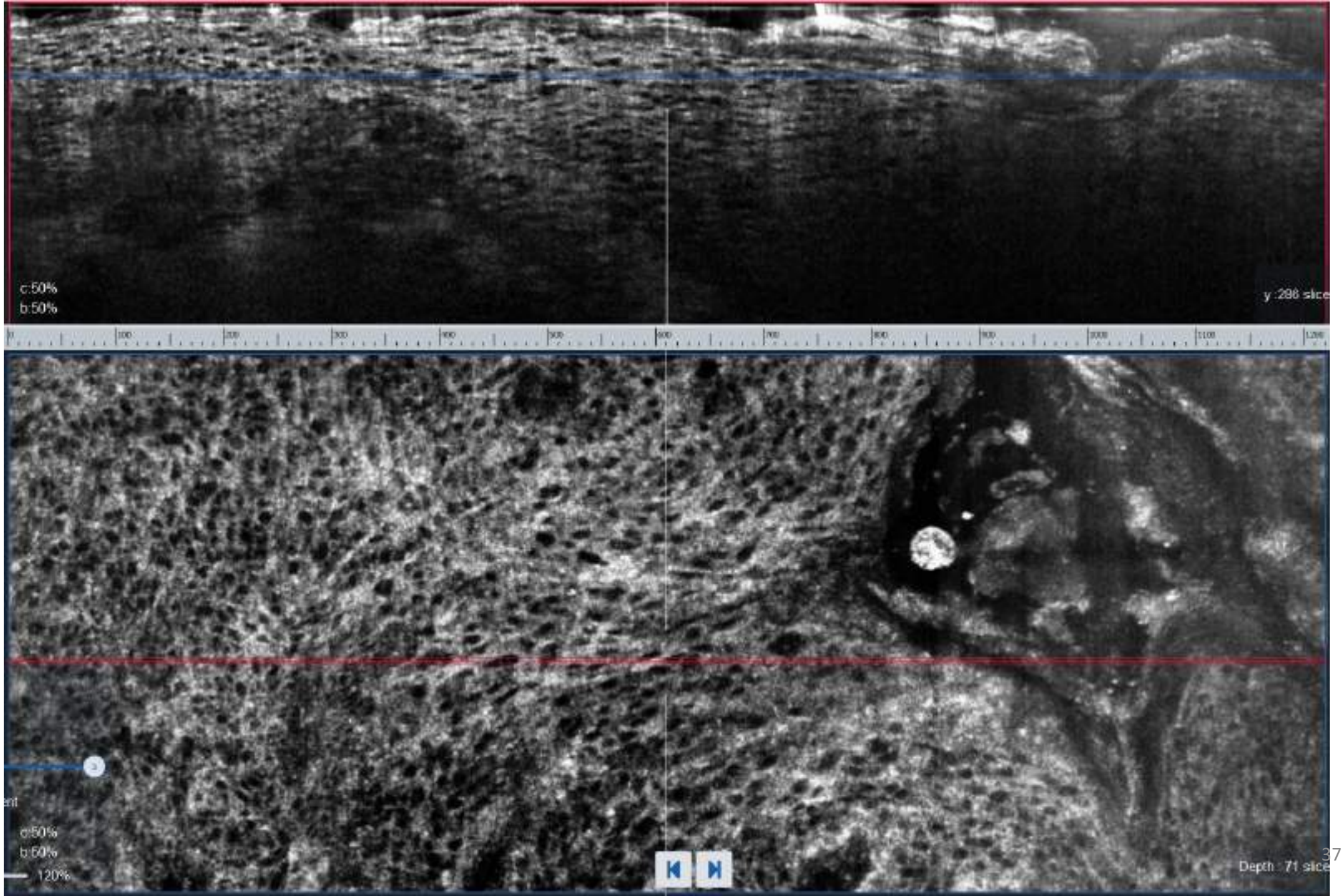
c:50%
b:50%
y :286 slice
c:50%
b:60%
120%
Depth : 71 slice

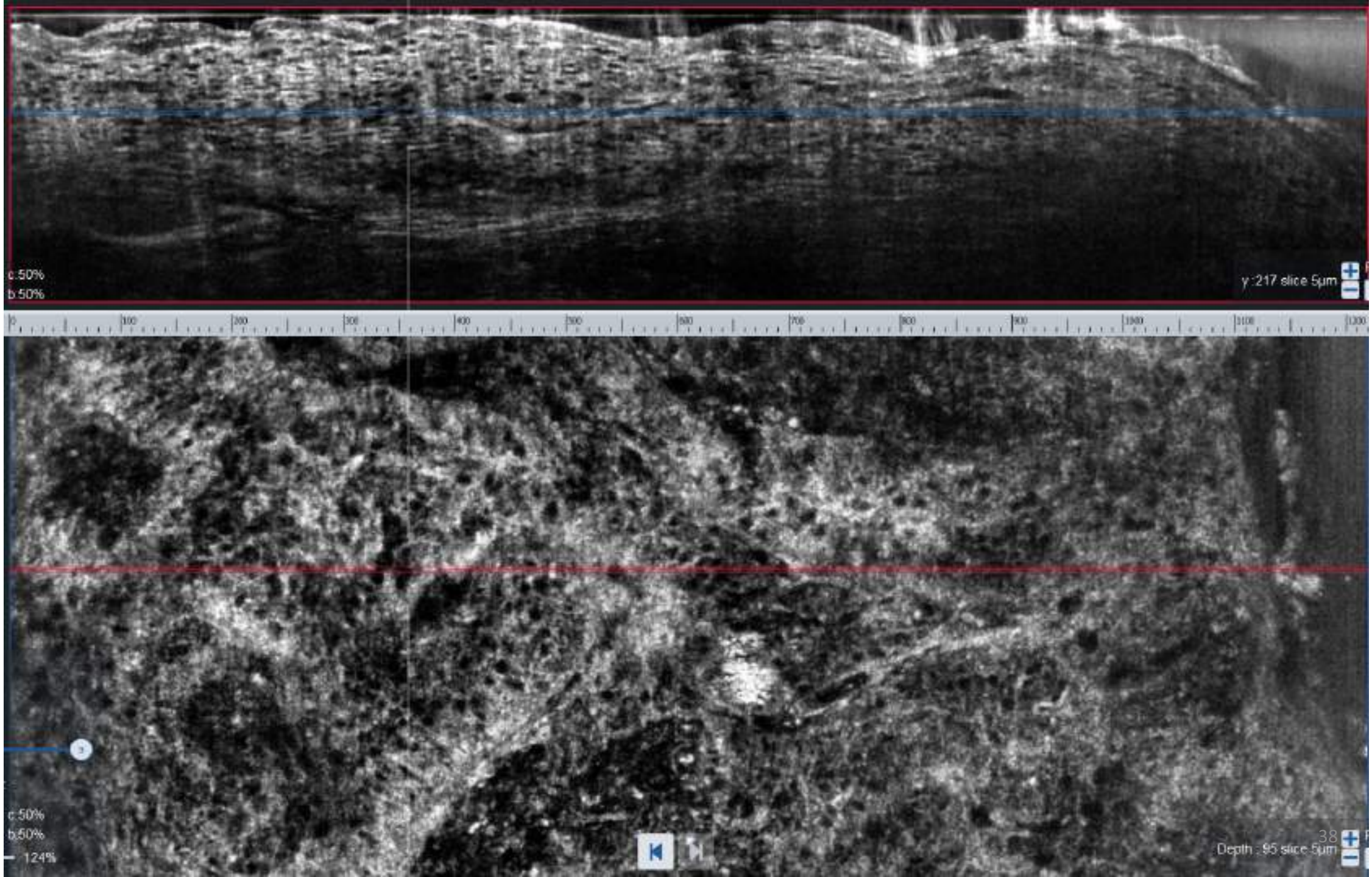
c:50%
b:50%
y :217 slice 5µm
c:50%
b:50%
124%
Depth : 95 slice 5µm

deepLive

by DAMAE MEDICAL

AI DETECTION OF BCC

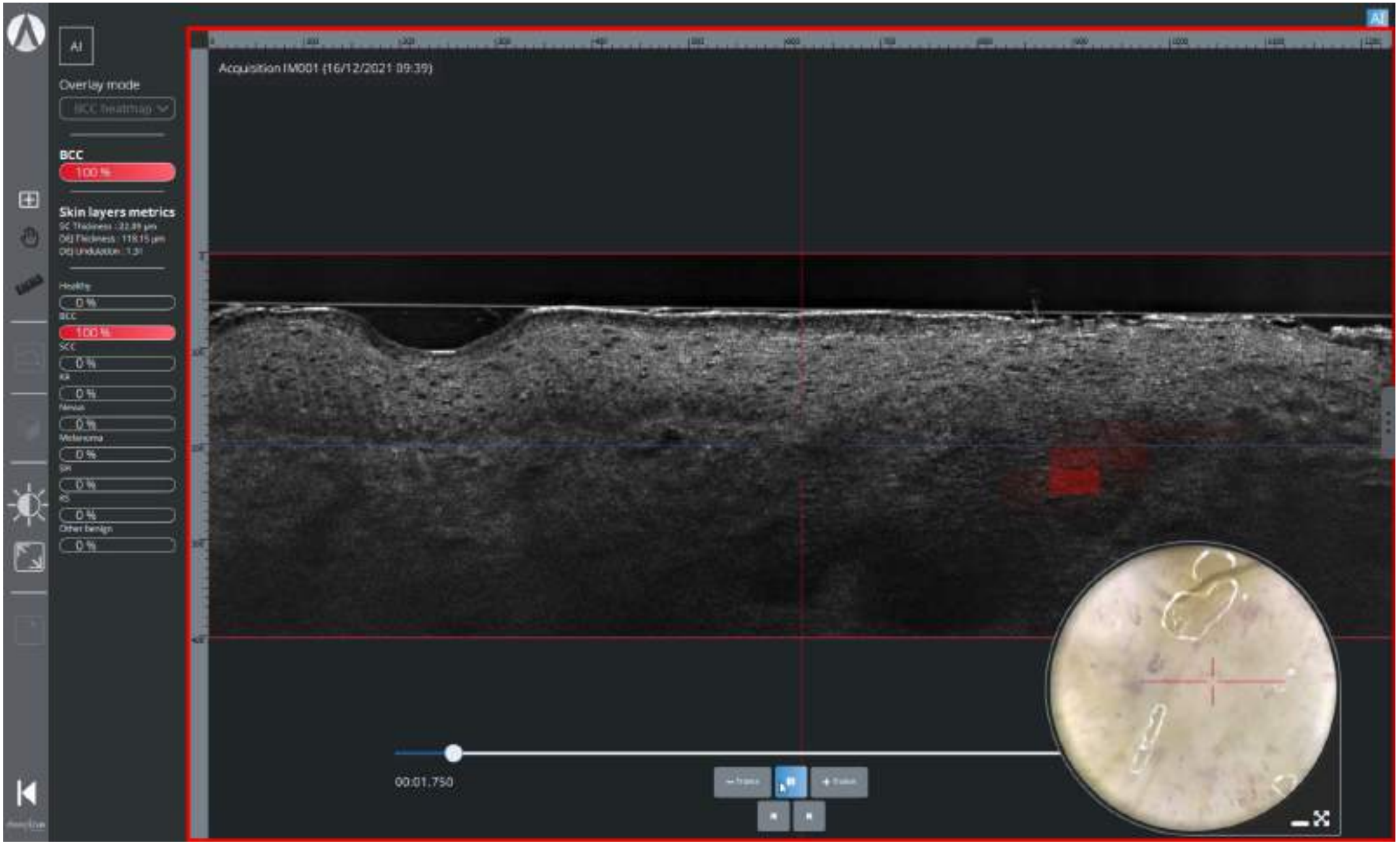

PRE-SURGICAL MARGINS ASSESSMENT

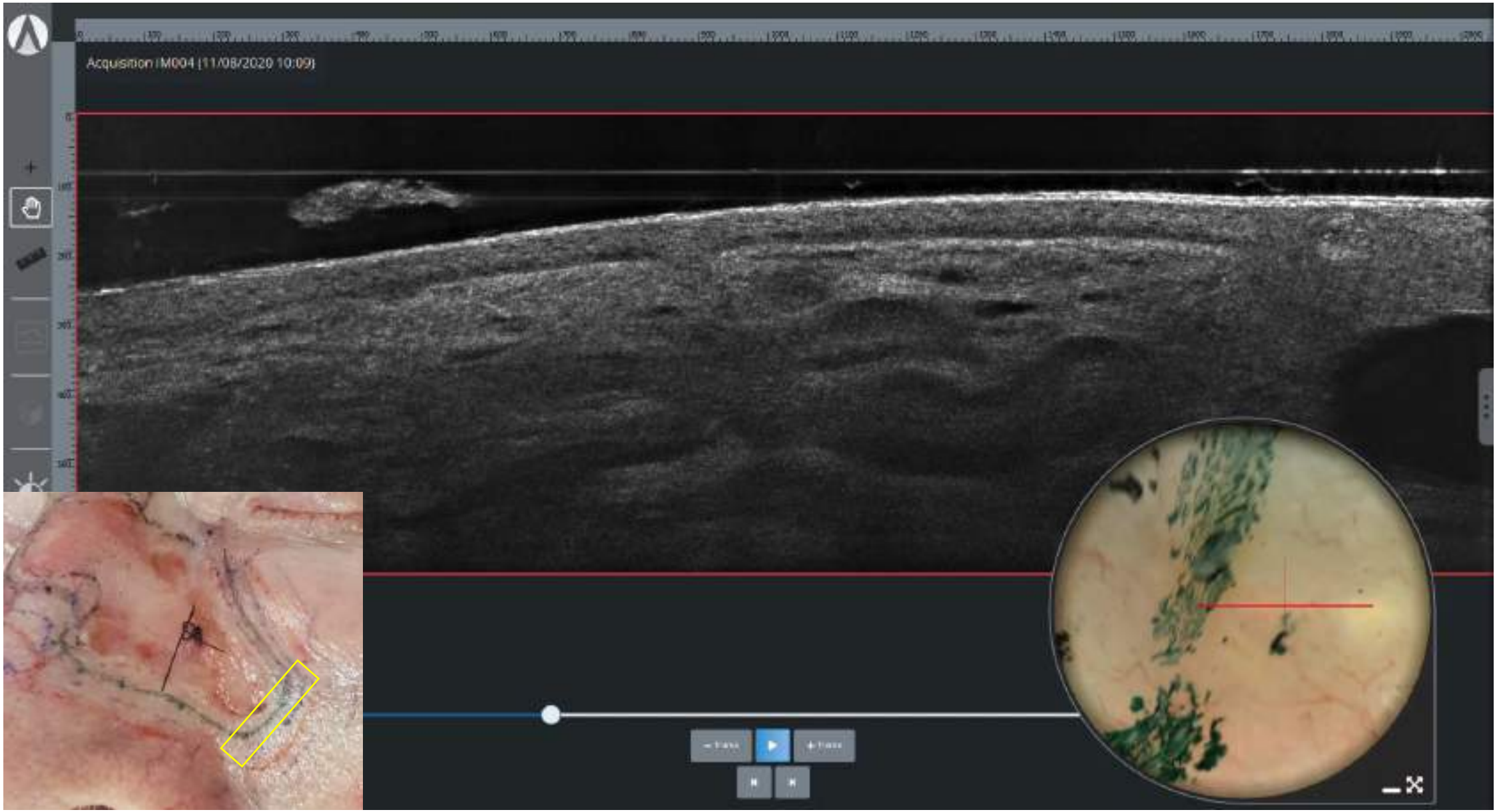

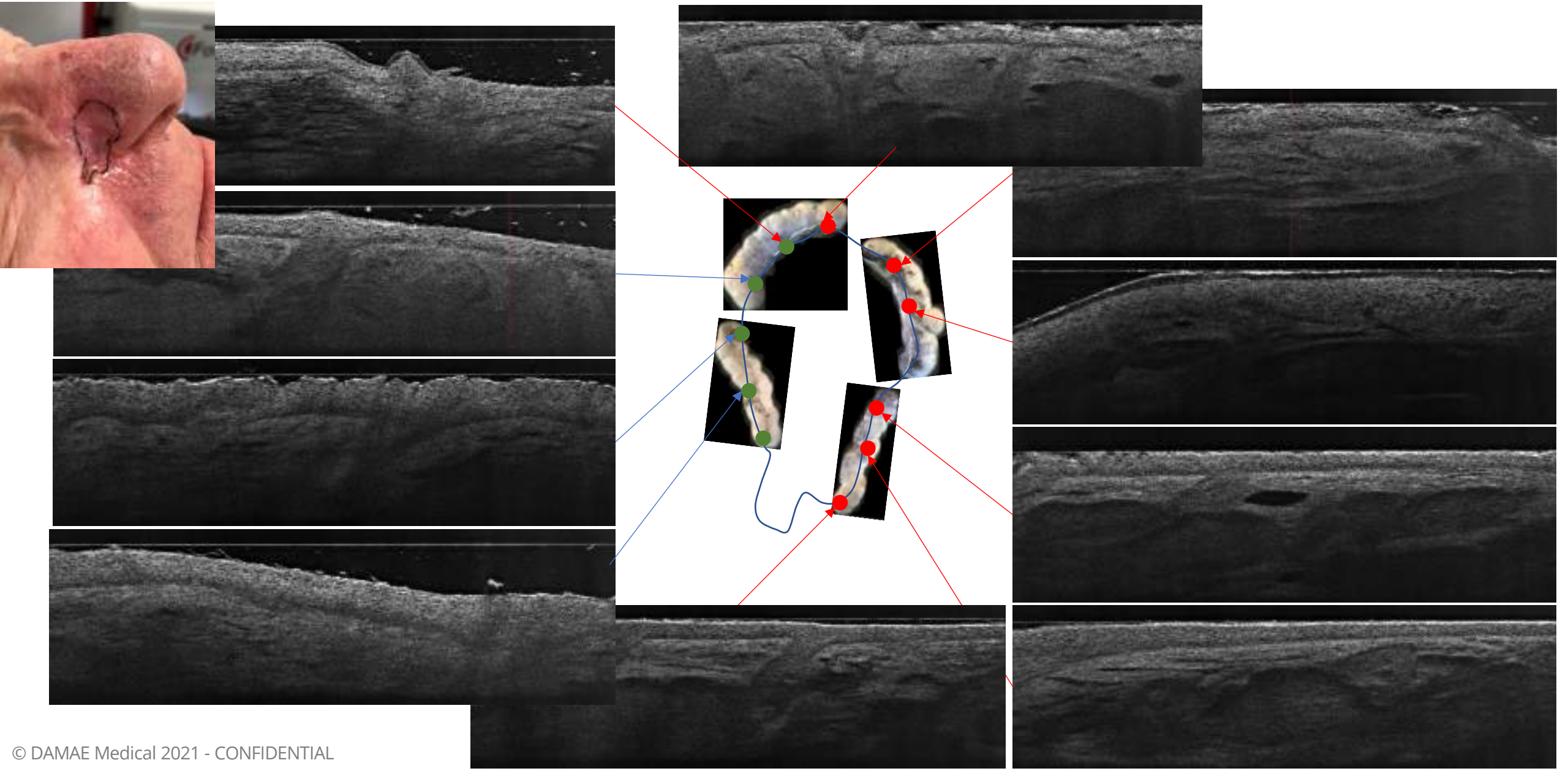

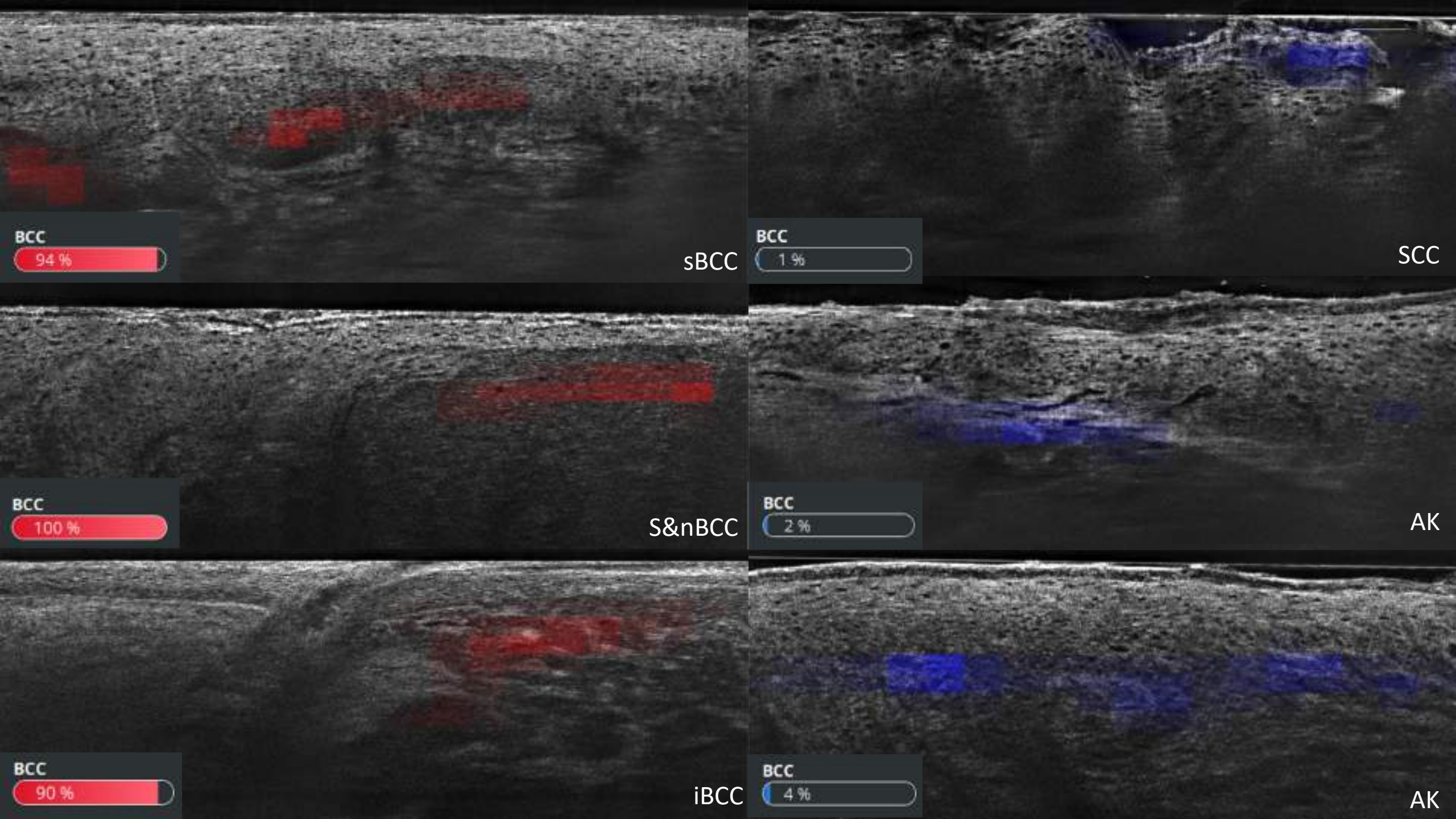
BCC
94 %
sBCC
BCC
1 %
SCC
BCC
100 %
S&nBCC
BCC
2 %
AK
BCC
90 %
iBCC
BCC
4 %
AK

Skin layers quantification

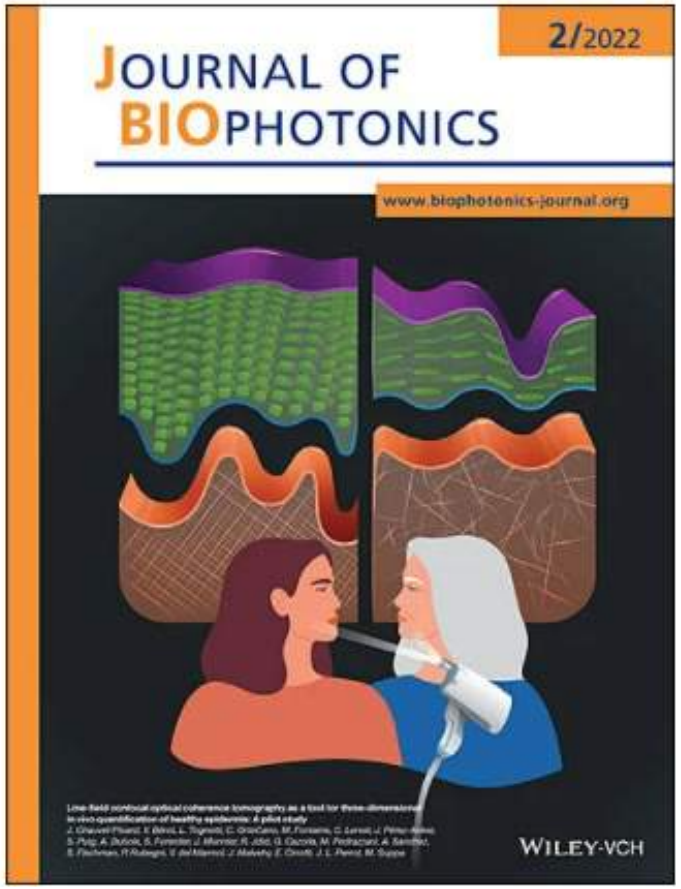

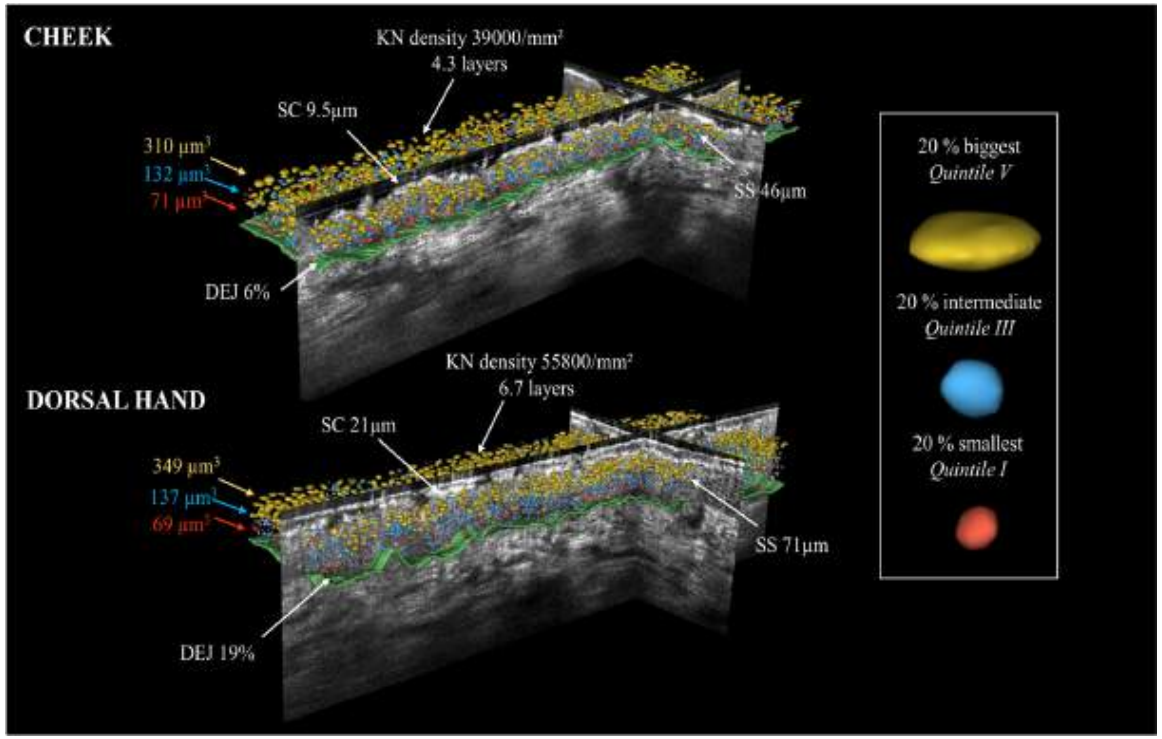

Chauvel-Picard J, Bérot V, Tognetti L, Orte Cano C, Fontaine M, Lenoir C, Pérez-Anker J, Puig S, Dubois A, Forestier S, Monnier J, Jdid R, Cazorla G, Pedrazzani M, Sanchez A, Fischman S, Rubegni P, Del Marmol V, Malvehy J, Cinotti E, Perrot JL, Suppa M. Line-field confocal optical coherence tomography as a tool for three-dimensional in vivo quantification of healthy epidermis: A pilot study. J Biophotonics. 2022 Feb;15(2):e202100236. doi: 10.1002/jbio.202100236. Epub 2021 Oct 21. PMID: 34608756.

Measurement of KC nuclei distribution (LC-OCT)

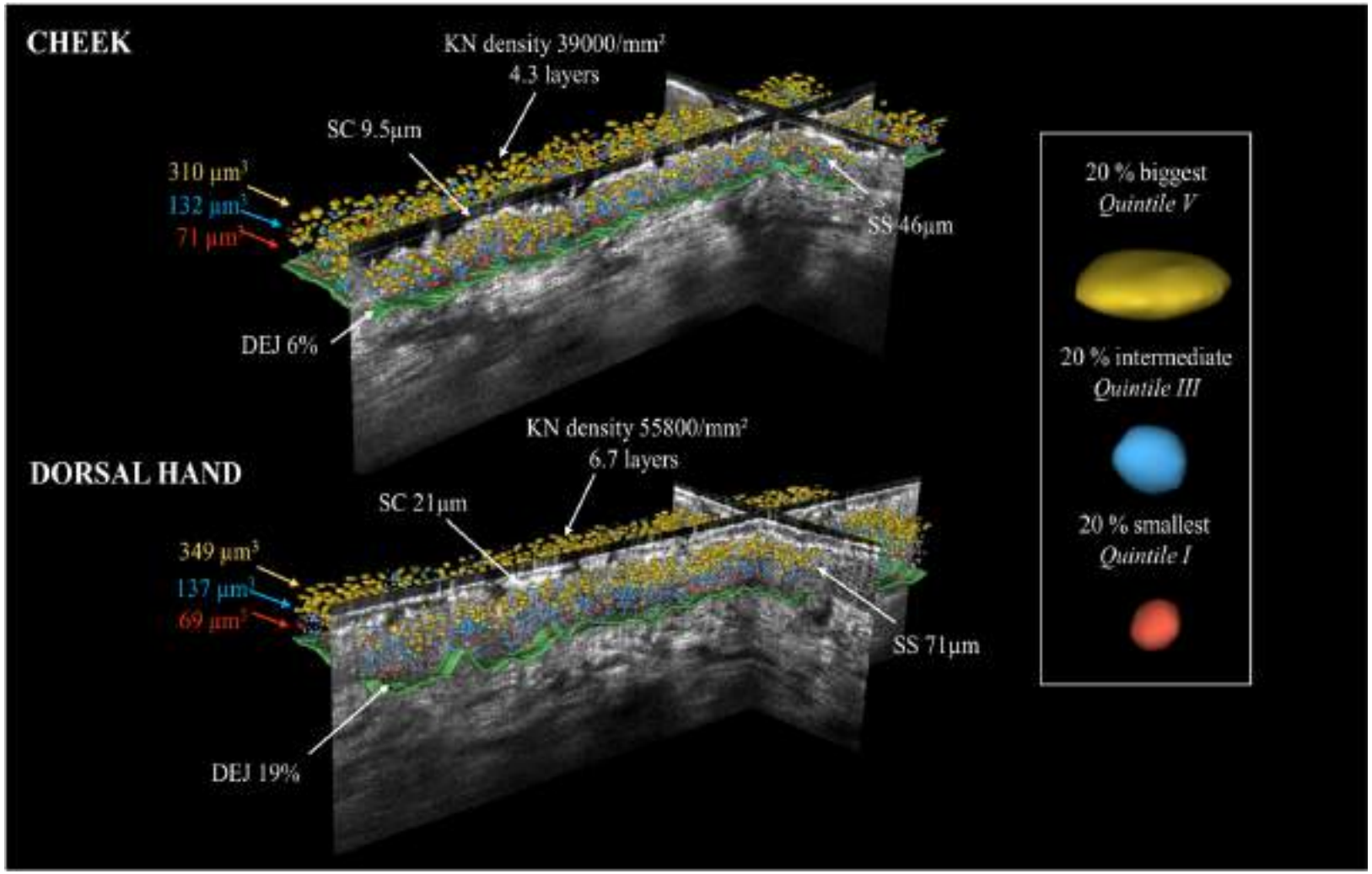

Keratinocyte nuclei distribution according to their volume (level of keratinocyte maturation) on the cheek and dorsal hand of the same study participant (21-year-old female, phototype II). Keratinocytes are illustrated in 3D and colored according to nuclei volume (red, quintile I including the smallest; blue, quintile III including the intermediate; yellow, quintile V including the biggest). The dermal- epidermal junction is depicted as a green layer (undulation index expressed in percentage). Three distinct layers are visible: a lower, red layer (just above the DEJ) containing small, immature basal keratinocytes; an intermediate, blue layer containing maturing keratinocytes; and an upper, yellow layer containing large, mature keratinocytes. DEJ, dermal epidermal junction; KN, keratinocytes; SC, stratum corneum; SS, stratum spinosum. Thicknesses (µm); nuclei volume (µm3); keratinocyte density (mm2) (Chauvel-Picard J et al)

Chauvel-Picard J, Bérot V, Tognetti L, Orte Cano C, Fontaine M, Lenoir C, Pérez-Anker J, Puig S, Dubois A, Forestier S, Monnier J, Jdid R, Cazorla G, Pedrazzani M, Sanchez A, Fischman S, Rubegni P, Del Marmol V, Malvehy J, Cinotti E, Perrot JL, Suppa M. Line-field confocal optical coherence tomography as a tool for three-dimensional in vivo quantification of healthy epidermis: A pilot study. J Biophotonics. 2022 Feb;15(2):e202100236. doi: 10.1002/jbio.202100236. Epub 2021 Oct 21. PMID: 34608756.

Measurement of photoageing: lineal confocal-OCT (LC-OCT)

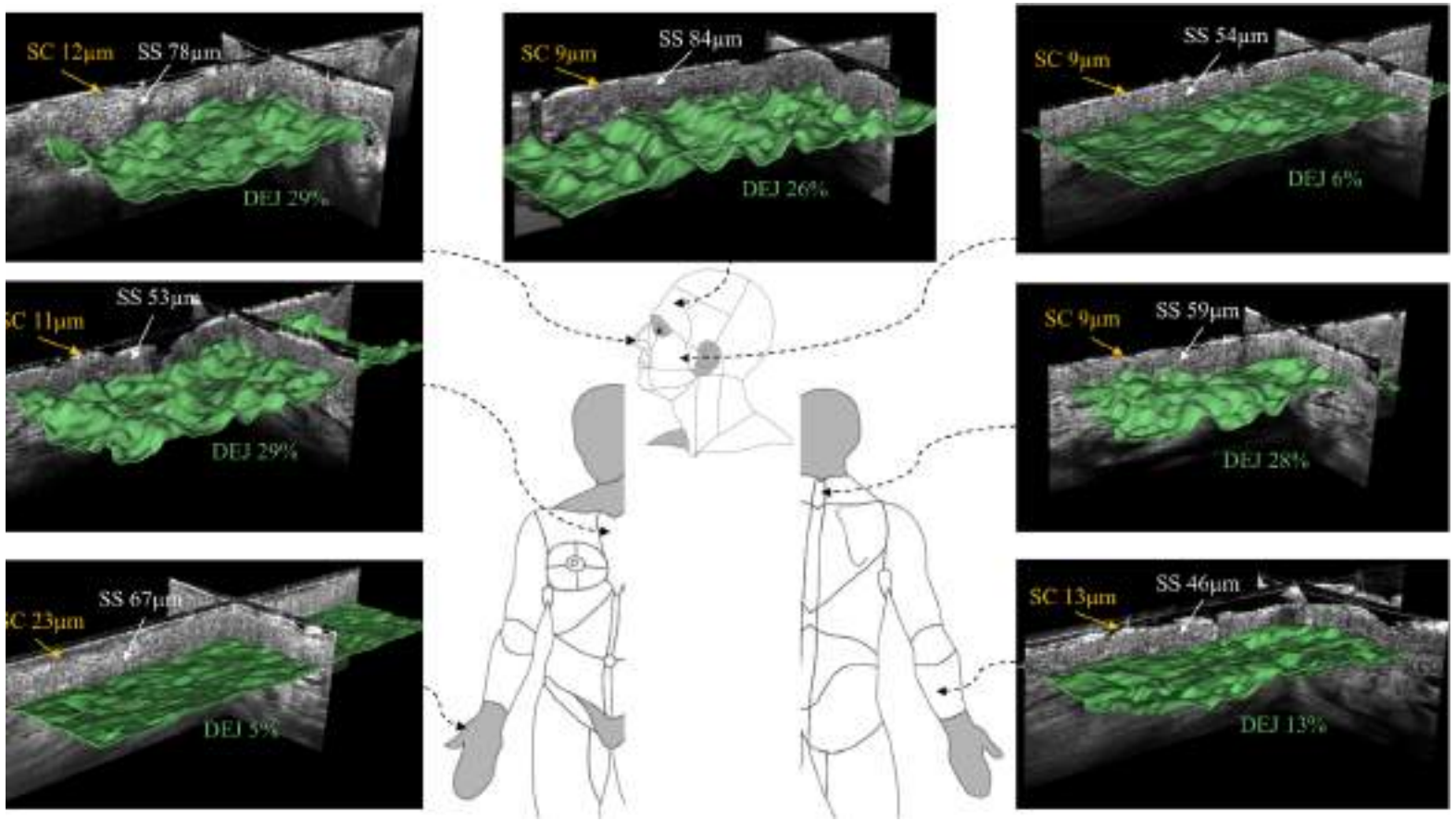

3D LC-OCT quantification of epidermal characteristics in seven body sites on the same subject (27-year-old female, phototype II). The thickness of stratum corneum (SC) and stratum spinosum (SS) are reported in µm, whereas the undulation of the dermal- epidermal junction (DEJ, green layer) is expressed in percentage (Chauvel-Picard J et al)

Chauvel-Picard J, Bérot V, Tognetti L, Orte Cano C, Fontaine M, Lenoir C, Pérez-Anker J, Puig S, Dubois A, Forestier S, Monnier J, Jdid R, Cazorla G, Pedrazzani M, Sanchez A, Fischman S, Rubegni P, Del Marmol V, Malvehy J, Cinotti E, Perrot JL, Suppa M. Line-field confocal optical coherence tomography as a tool for three-dimensional in vivo quantification of healthy epidermis: A pilot study. J Biophotonics. 2022 Feb;15(2):e202100236. doi: 10.1002/jbio.202100236. Epub 2021 Oct 21. PMID: 34608756.

scientific reports

OPEN

Non-invasive scoring of cellular atypia in keratinocyte cancers in 3D LC-OCT images using Deep Learning

Sébastien Fischman[1]✉, Javiera Pérez-Anker[2,3], Linda Tognetti[4], Angelo Di Naro[4], Mariano Suppa[5,6,7], Elisa Cinotti[4,6], Théo Viel[1], Jilliana Monnier[6,8], Pietro Rubegni[4], Véronique del Marmol[5], Josep Malvehy[2,3], Susana Puig[2,3], Arnaud Dubois[9] & Jean-Luc Perrot[10]

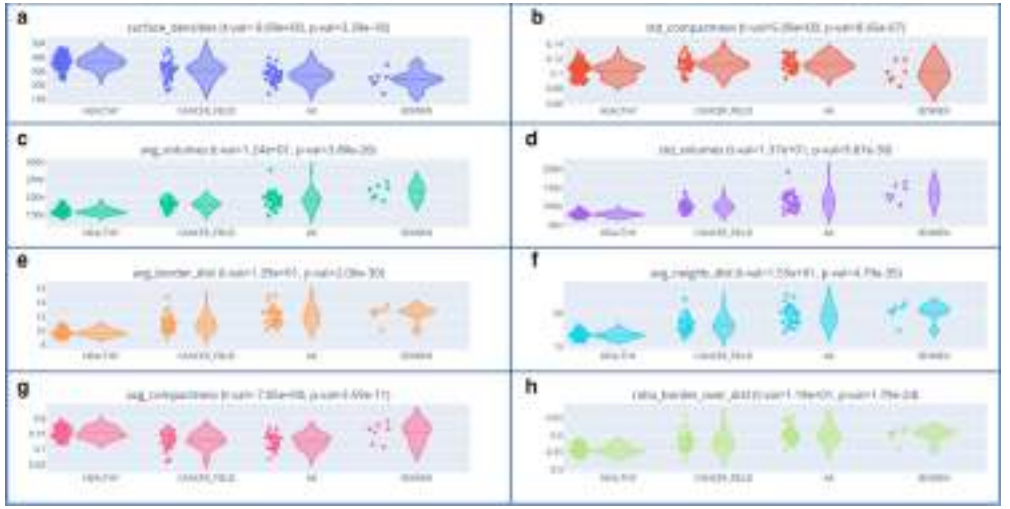

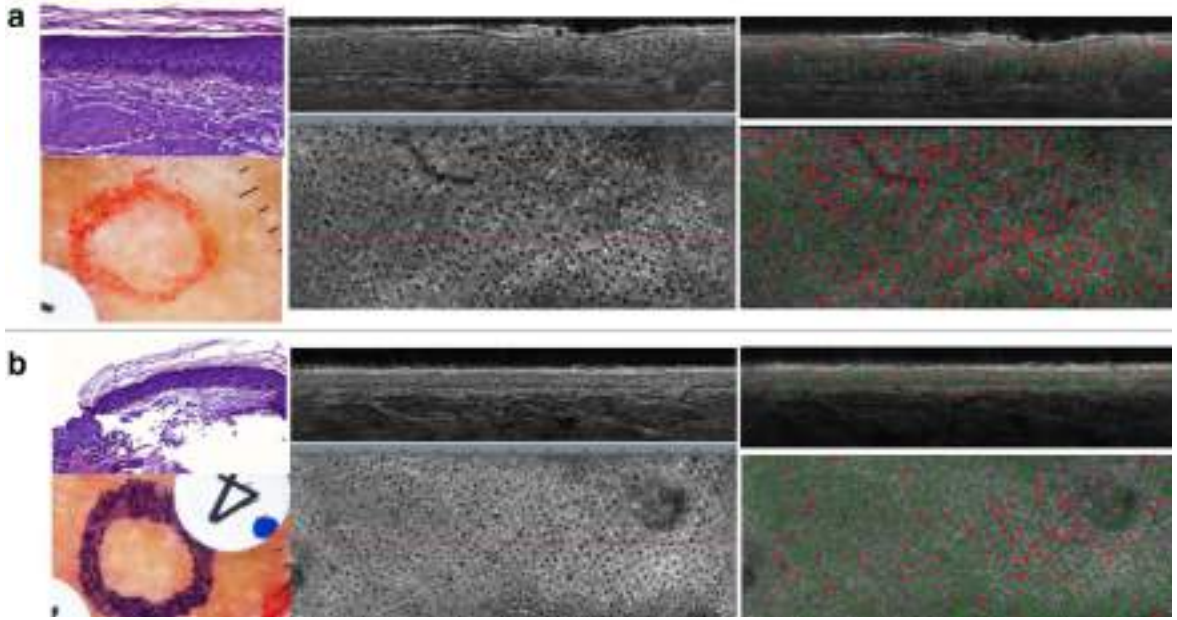

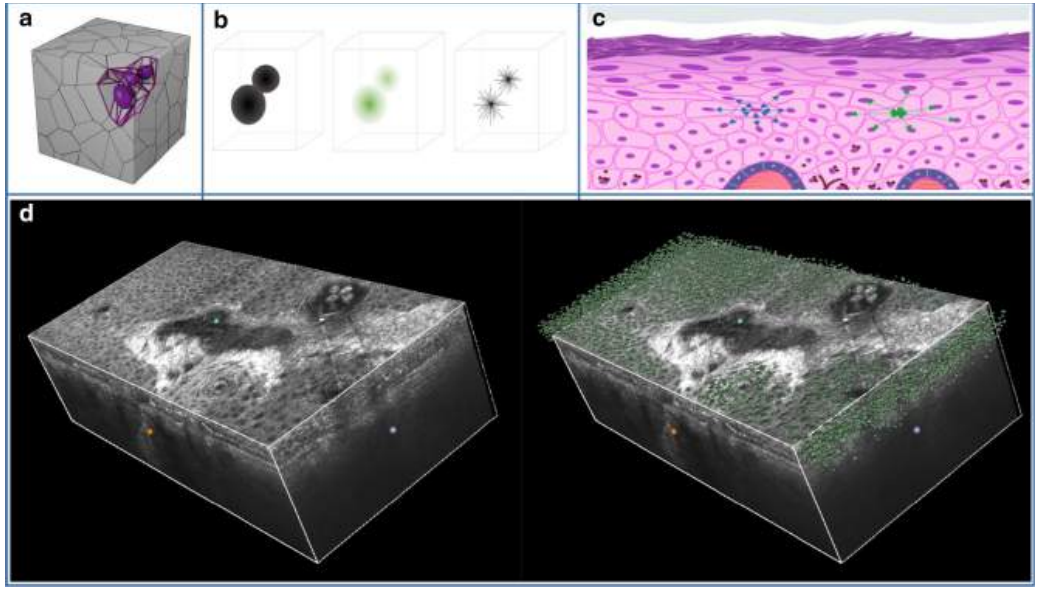

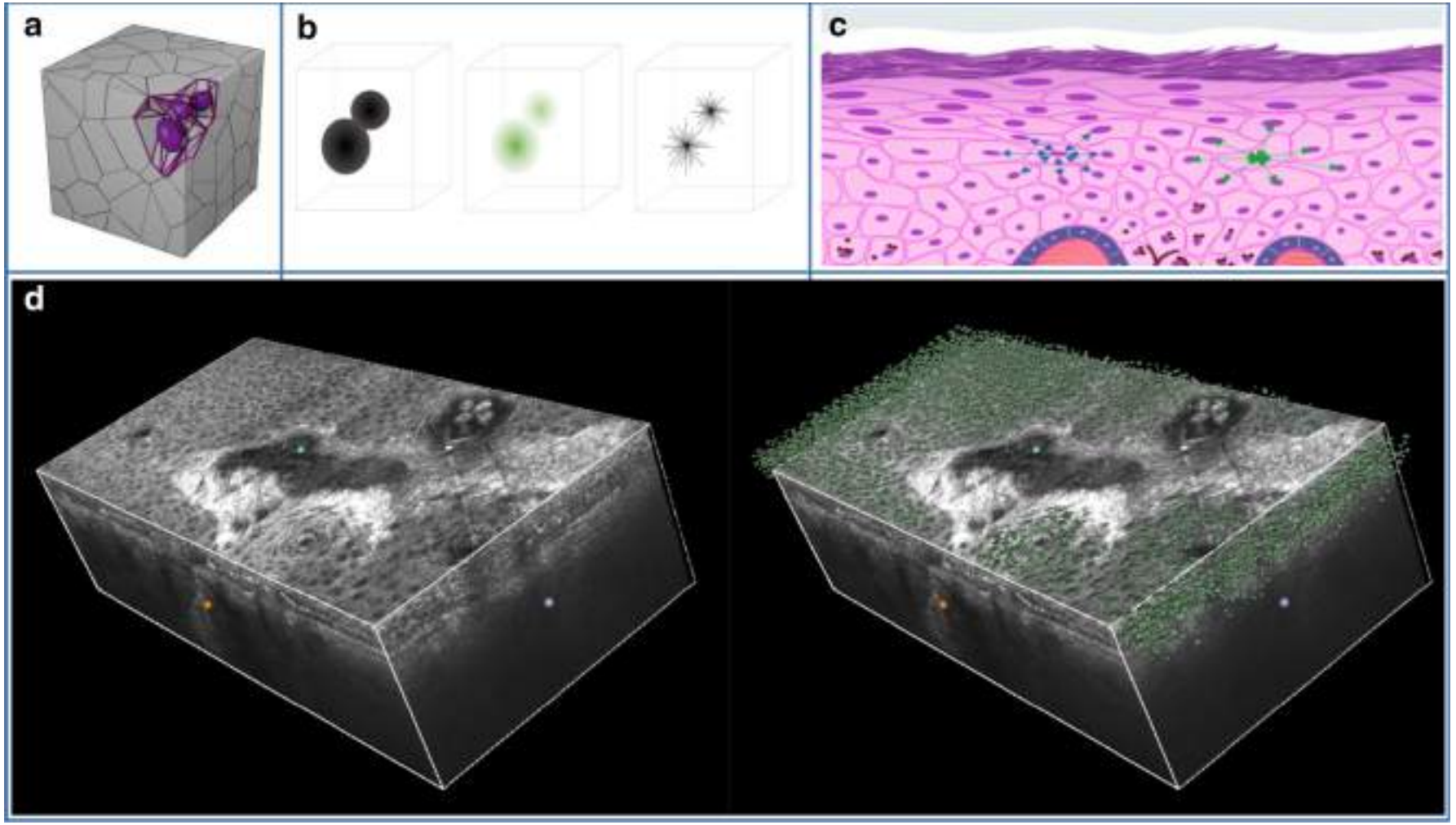

- 3.7 million nuclei detected by the Deep Learning model (2.5 millions healthy images, 491000 in AK, images= 630000 in fields of cancerization and 95000 in SCC.

- Atypia of KC: larger nuclei, less spherical, hetereogeneous

Measurement of KC nuclei distribution (LC-OCT)

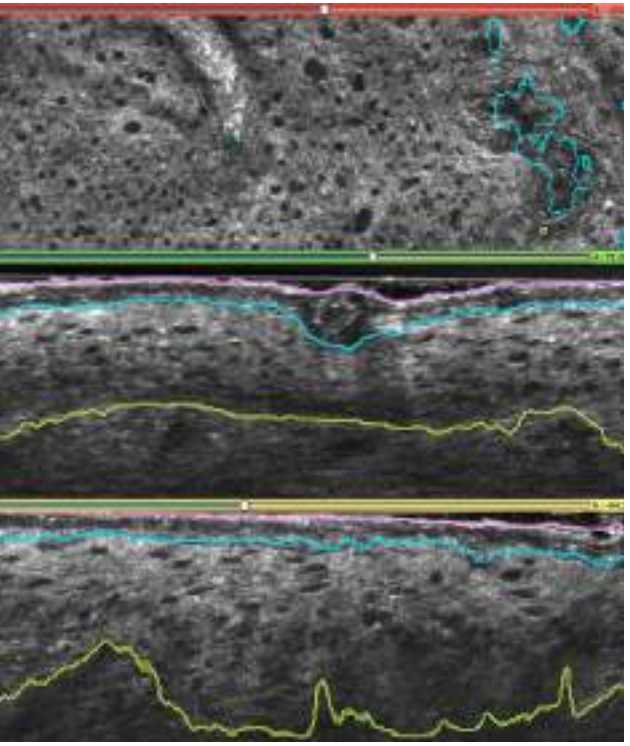

Skin layers segmentation

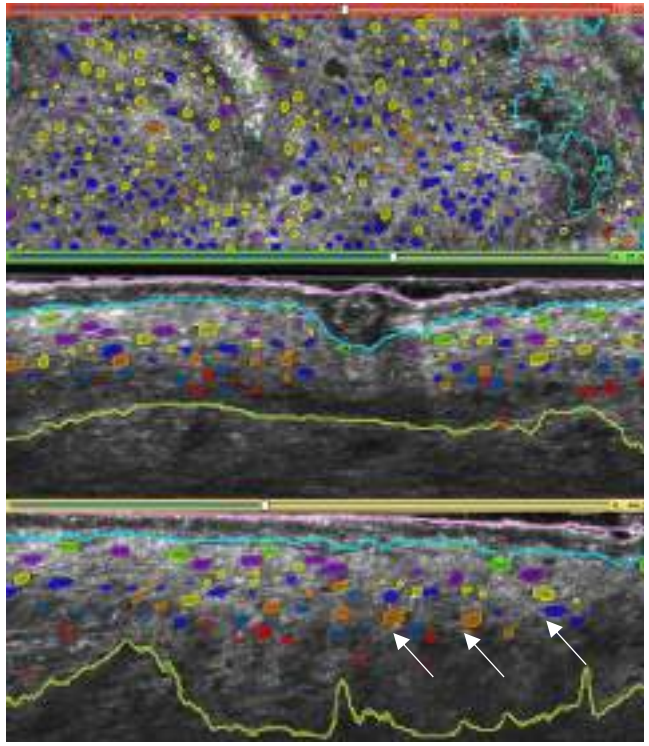

Nuclei per layers (3D)
Green: 1st top layer
Blue: middle layer
Red: bottom layer

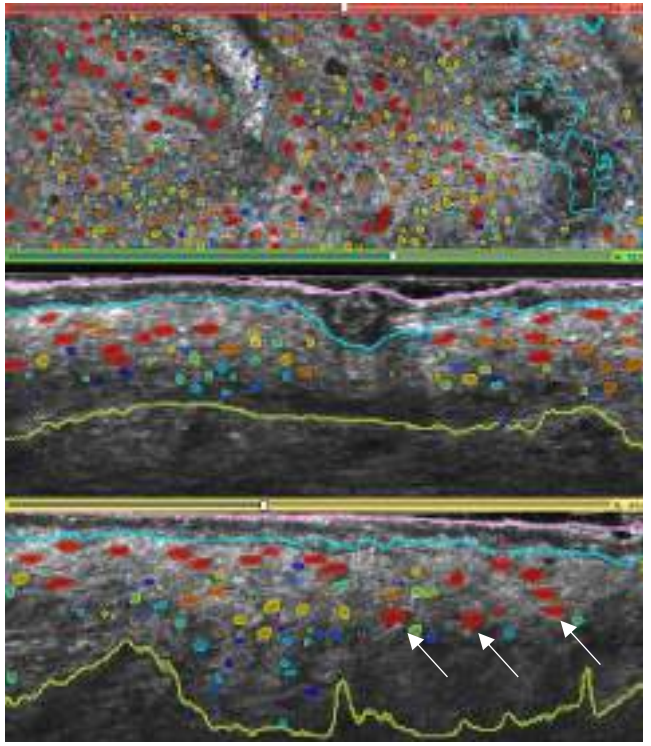

Nuclei per size (volume)
red: largest nuclei
Green/yellow: intermediate
blue: smallest

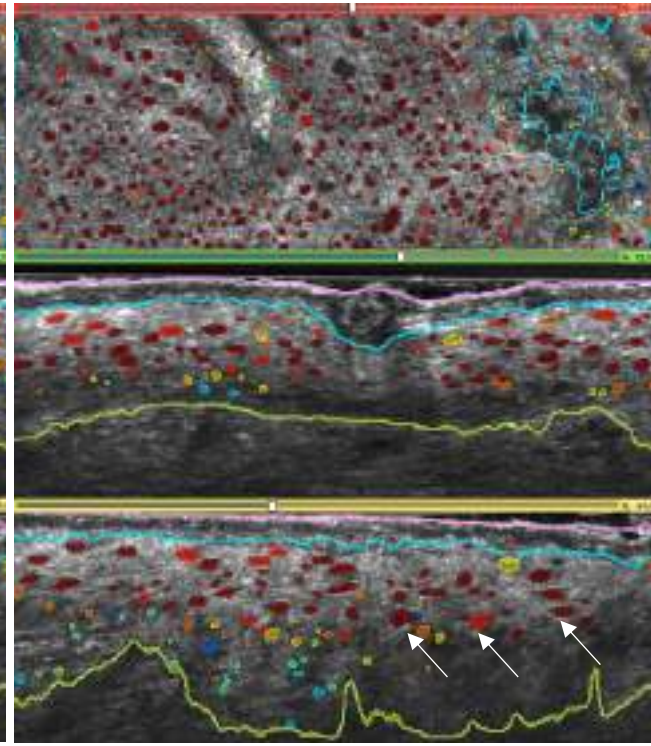

Nuclei per atypia (AI score)
red: highest atypia
Green/yellow: intermediate
blue: smallest atypia

- In the combined images of this study, a total of more than 3.7 million nuclei were detected by the Deep Learning model with 2.5 millions nuclei from healthy images, 491000 in AK, 630000 in fields of cancerization and 95000 in Bowens.
- Atypia of KC: larger nuclei, less spherical, hetreogeneous

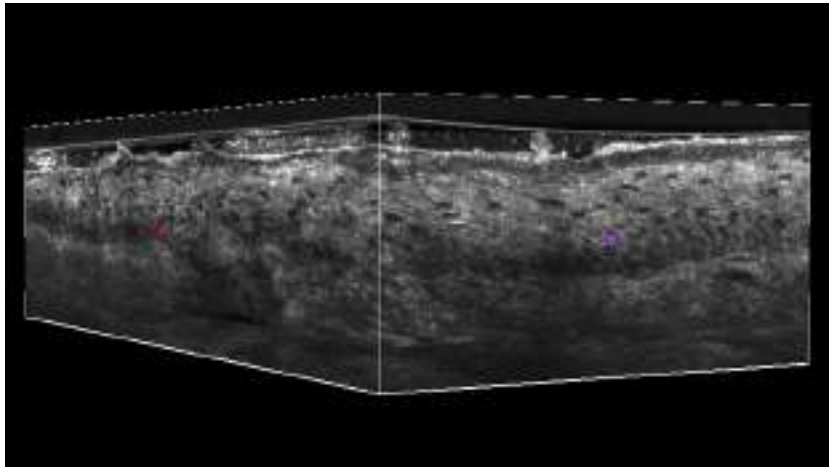

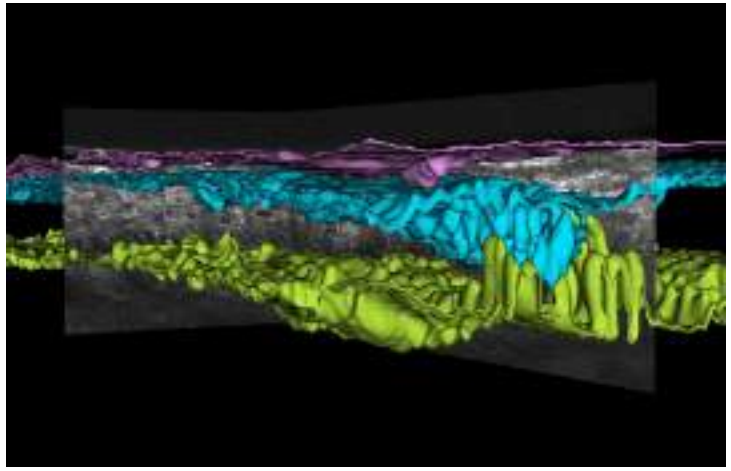

Skin layers segmentation

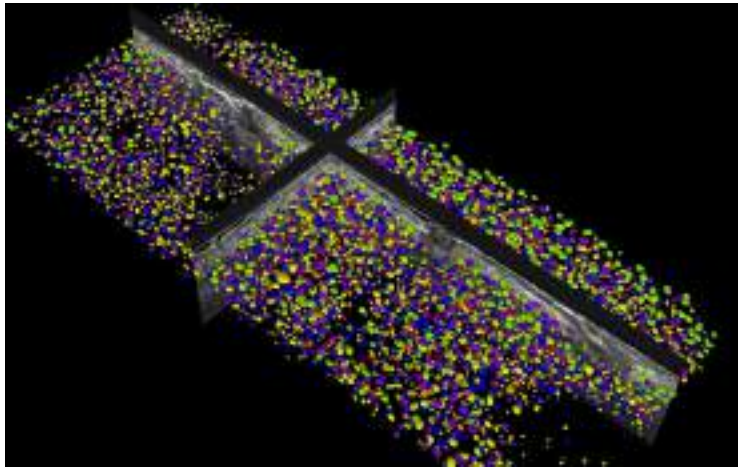

Nuclei per layers (3D)
Green: 1st top layer / Blue: middle layer /
Red: bottom layer

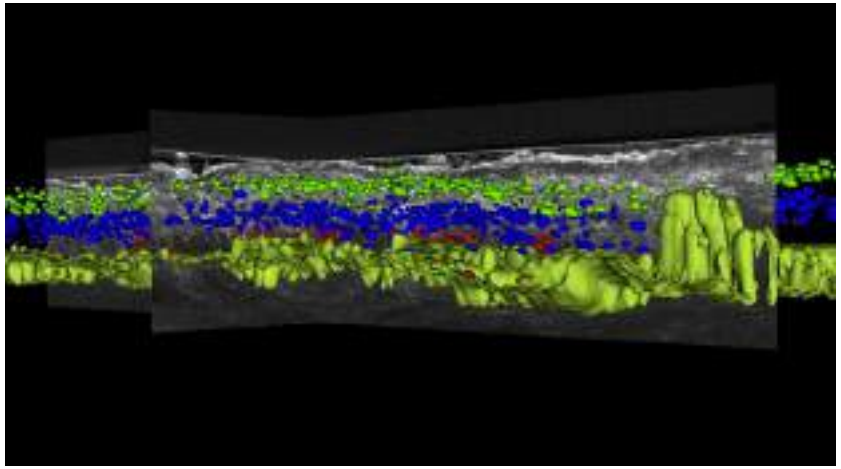

Nuclei per layers (3D)
Green: 1st top layer
Blue: middle layer
Red: bottom layer

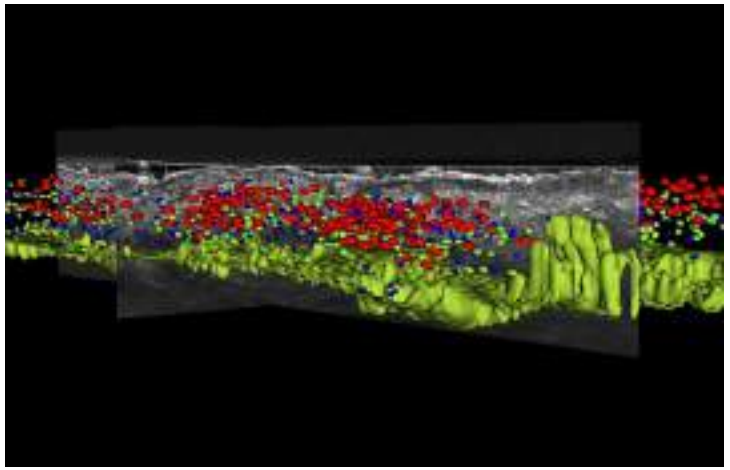

Nuclei per size (volume)
red: largest nuclei
Green: intermediate
blue: smallest

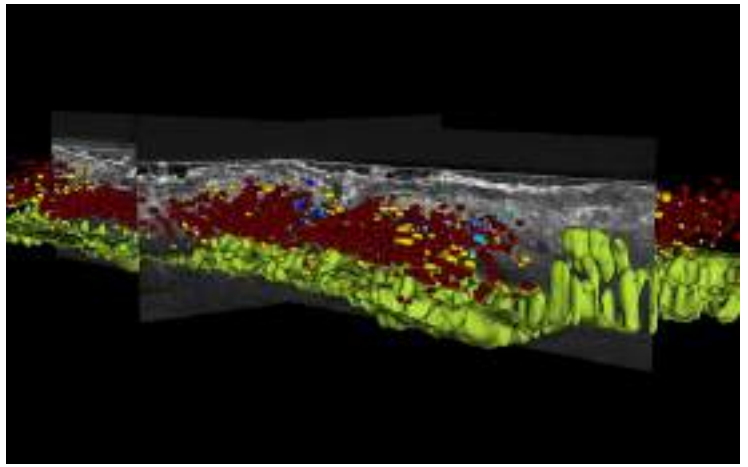

Nuclei per atypia (AI score)
red: highest atypia
Green/yellow: intermediate
blue: smallest atypia

Examples of live protrusion quantification

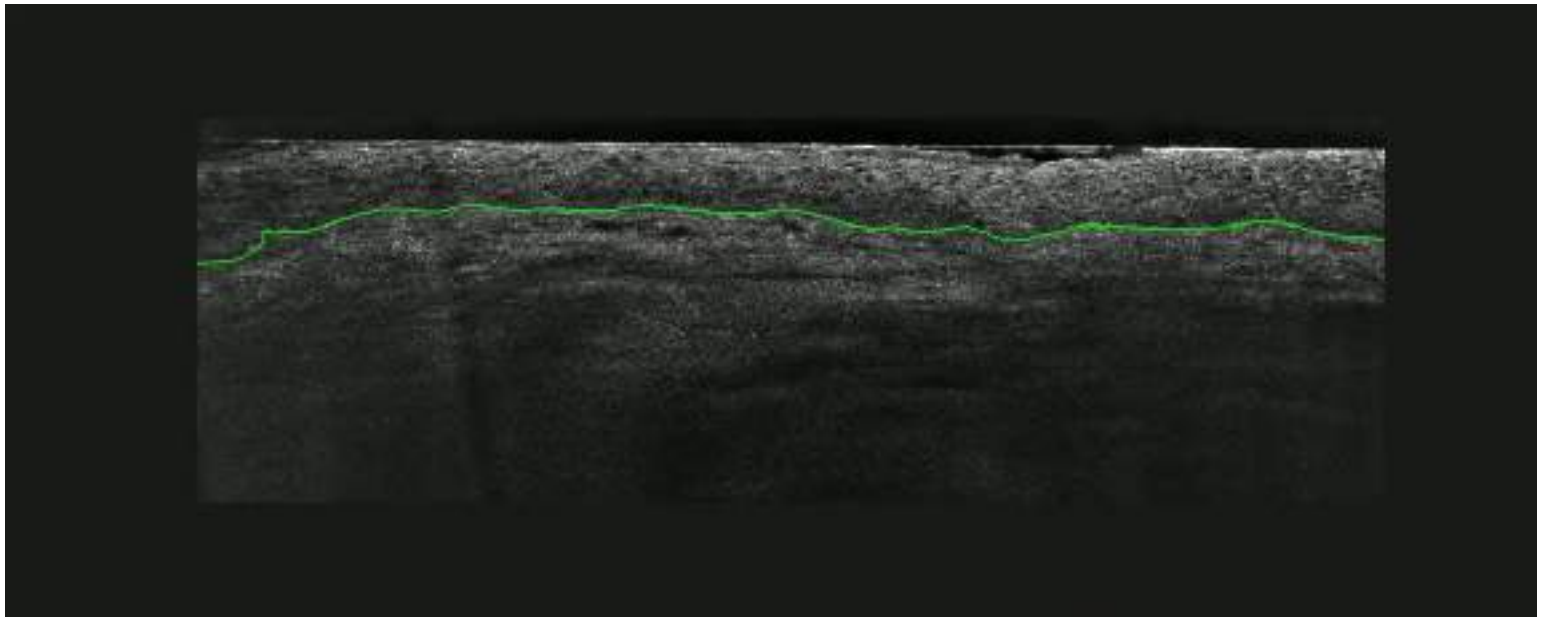

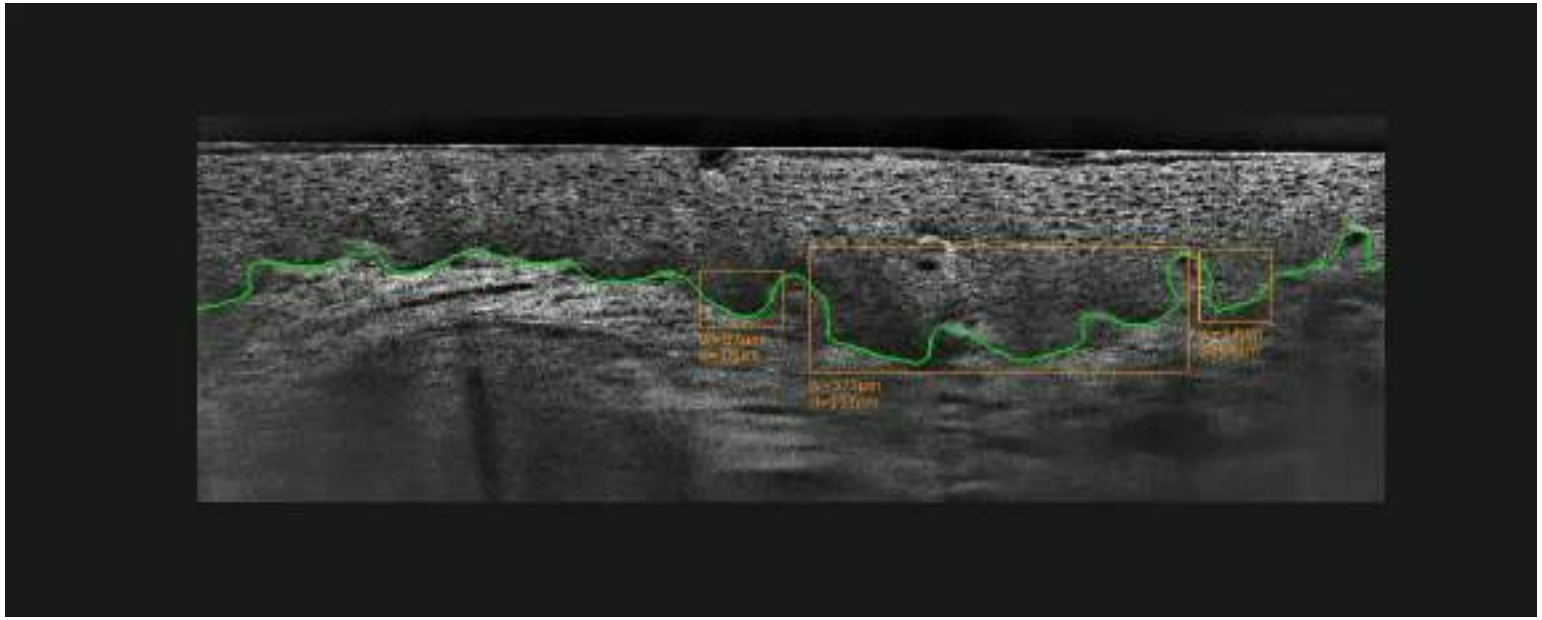

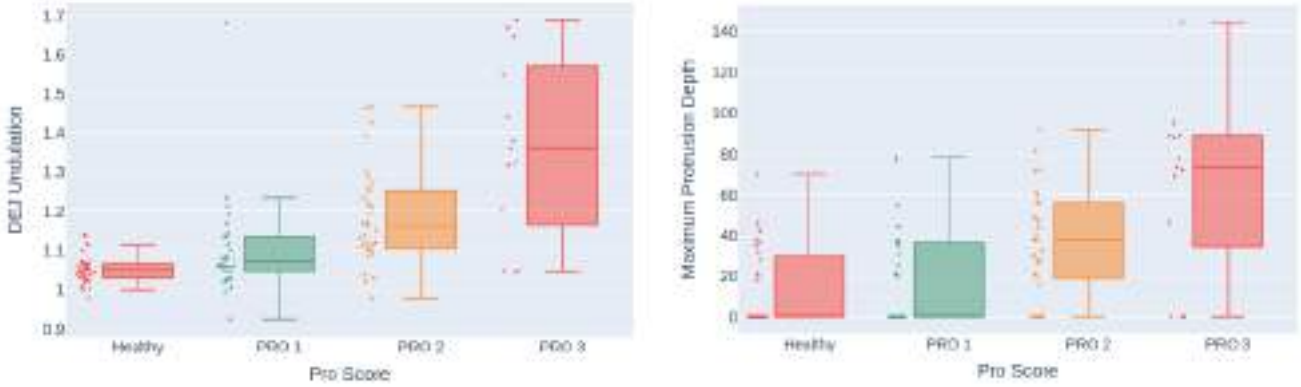

(a) Undulation. (b) Maximum protrusion depth.

Predicted Label

Ground truth	PRO I	PRO II	PRO III
PRO I	20	10	0
PRO II	4	28	1
PRO III	3	1	9

Table 2. Confusion matrix of the PRO Scoring model.

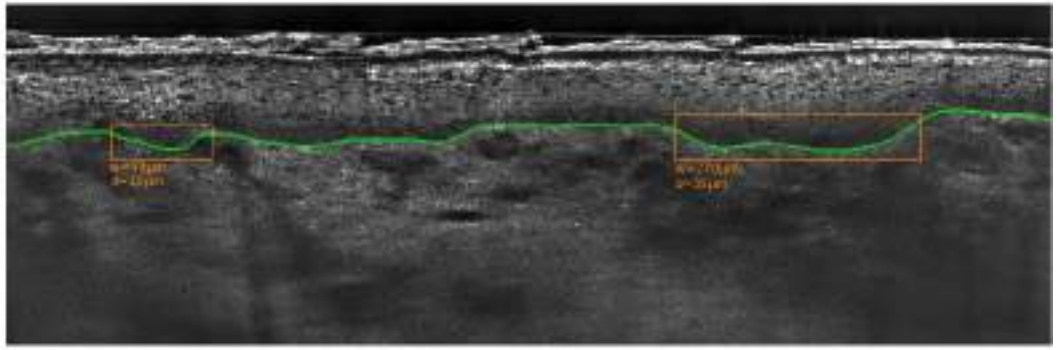

-> Grade based on undulation : [PRO 1]
JDE thickness : 80 µm
JDE undulation : 1.116

-> Grade based on undulation : [PRO 2]
JDE thickness : 101 µm
JDE undulation : 1.267

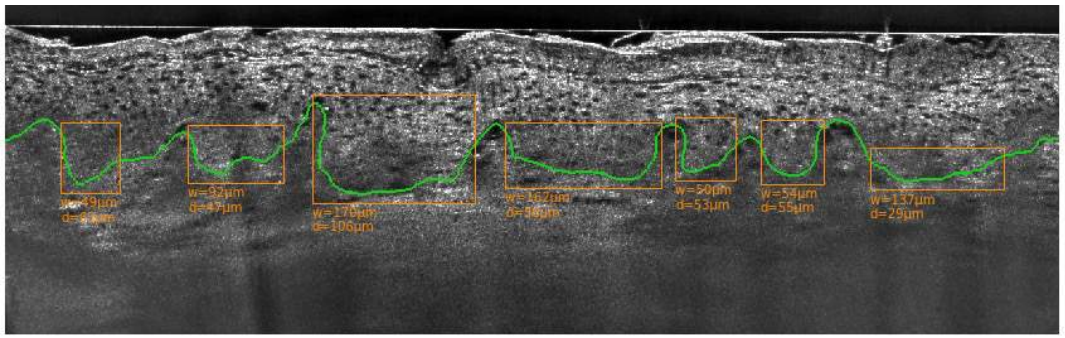

-> Grade based on undulation : [PRO 3]
JDE thickness : 105 µm
JDE undulation : 1.604

Conclusions

- No reliable clinical criteria to identify “high-risk” AKs
- Proliferative patterns of Aks associated to resistance to Tx and SCC
- LC-OCT aids in the identification of PRO AKs
- LC-OCT aids in the identification of SCC
- AI and LC-OCT to quantify the skin changes in AKs and SCC

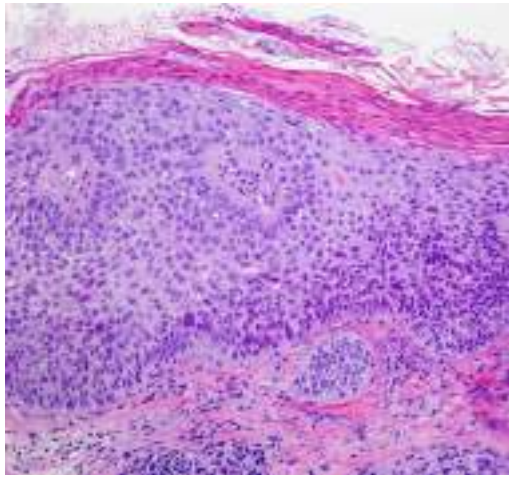

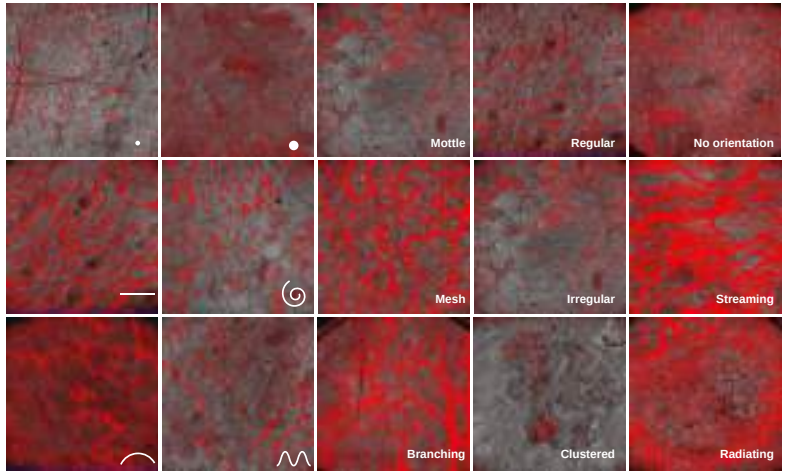

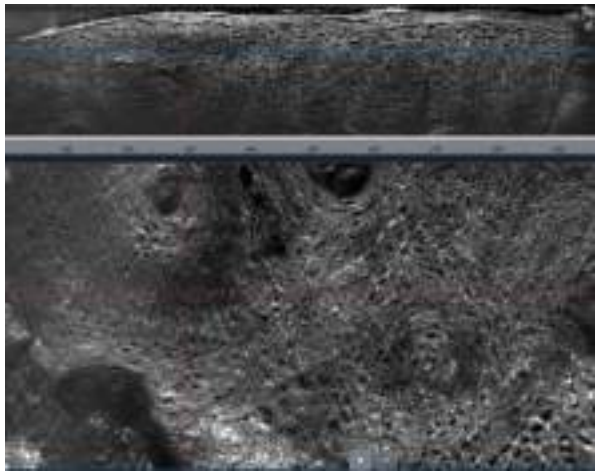

Dermatology Department Hospital Clinic

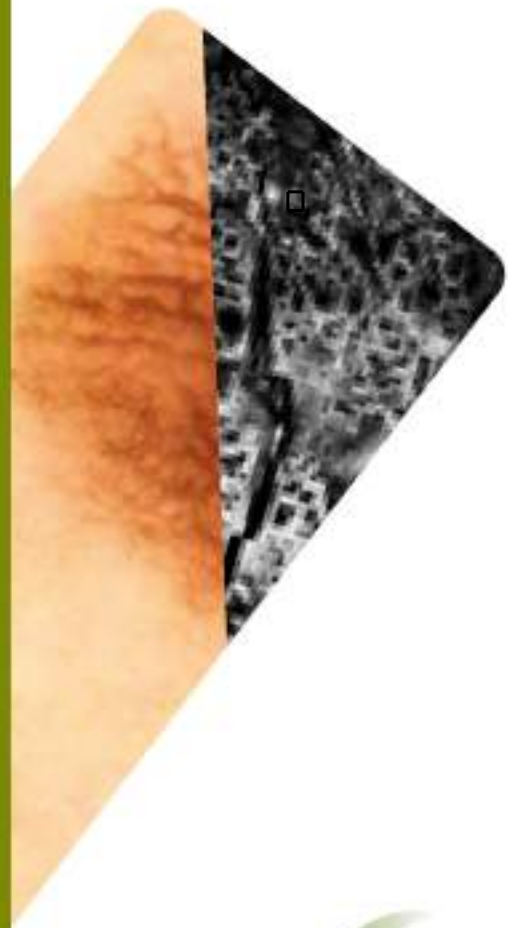

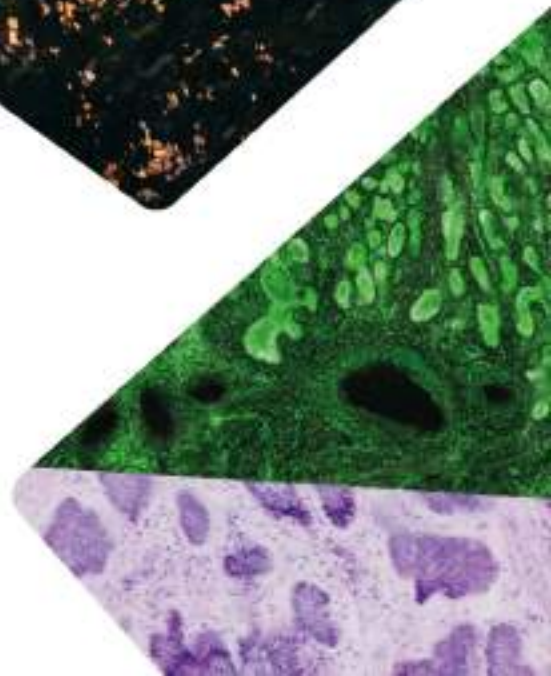

Hybrid Congress

3rd World Congress on Confocal Microscopy

June, 1-3, 2023
Barcelona, Spain

Save the date!

ICG International Confocal Group

Organizing Committee
Salvador González
Josep Malvehy
Giovanni Pellacani
Javiera Pérez-Anker
Susana Puig

https://confocalcongress.bocemtium.com
#confocalcongress

- Nuevos **criterios diagnósticos en tumores y otras enfermedades de la piel.**
- **Desarrollo de la tecnología** y su **combinación con otras técnicas de diagnóstico no invasivo** y la **inteligencia artificial.**
- **Kahoots para jugar** después de cada bloque de temas
- **e-pósters para su discusión** y la votación para elegir al premiado será entre todos los asistentes.

Profesorado

- **Zoe Apalla.** *Servicio de Dermatología. Universidad Aristóteles. Tesalónica. Grecia*
- **Giuseppe Argenziano.** *Servicio de Dermatología. Universidad de Campania. Nápoles. Italia*
- **José Bañuls Roca.** *Servicio de Dermatología. Hospital General Universitario. Alicante*
- **Cristina Carrera Álvarez.** *Servicio de Dermatología. Hospital Clínic. Barcelona*
- **Natalia Espinosa.** *Servicio de Dermatología. Hospital Clínic. Barcelona*
- **Lara Ferrándiz Pulido.** *Servicio de Dermatología. Hospital Universitario Virgen de la Macarena. Sevilla*
- **Reyes Gamo Villegas.** *Servicio de Dermatología. Fundación Hospital Alcorcón. Madrid*
- **Aimilios Lallas.** *Servicio de Dermatología. Universidad Aristóteles. Tesalónica. Grecia*
- **Caterina Longo.** *Universidad de Módena y Reggio Emilia. Modena, Italia*
- **Josep Malvehy Guilera.** *Servicio de Dermatología. Hospital Clínic. Barcelona*
- **David Moreno Ramírez.** *Servicio de Dermatología. Hospital Universitario Virgen de la Macarena. Sevilla*
- **Javiera Pérez Anker.** *Servicio de Dermatología. Hospital Clínic. Barcelona*
- **Sebastian Podlipnik.** *Servicio de Dermatología. Hospital Clínic. Barcelona*
- **Susana Puig Sardà.** *Servicio de Dermatología. Hospital Clínic. Barcelona*
- **Gissele Rezze.** *Servicio de Dermatología. Hospital Clínic. Barcelona*
- **Luc Thomas.** *Servicio de Dermatología. Centro Hospitalario Universitario Lyon-Sud. Lyon. Francia*
- **Pedro Zaballos Diego.** *Servicio de Dermatología. Hospital de Sant Pau i Santa Tecla. Tarragona*